

GALEX Ultraviolet Photometry of Globular Clusters in M31: Three Year Results and a Catalog

Soo-Chang Rey^{1,2,3}, R. Michael Rich⁴, Sangmo T. Sohn^{2,5}, Suk-Jin Yoon², Chul Chung²,
Sukyoung K. Yi², Young-Wook Lee², Jaehyon Rhee^{2,3}, Luciana Bianchi⁶, Barry F.
Madore⁷, Kyungsook Lee¹, Tom A. Barlow³, Karl Forster³, Peter G. Friedman³, D.
Christopher Martin³, Patrick Morrissey³, Susan G. Neff⁸, David Schiminovich⁹, Mark
Seibert³, Todd Small³, Ted K. Wyder³, Jose Donas¹⁰, Timothy M. Heckman¹¹, Bruno
Milliard¹⁰, Alex S. Szalay¹¹, Barry Y. Welsh¹²

ABSTRACT

We present ultraviolet (UV) photometry of M31 globular clusters (GCs) found in 23 *Galaxy Evolution Explorer* (GALEX) images covering the entirety of M31. We detect 485 and 273 GCs (and GC candidates) in the near-ultraviolet (NUV; $\lambda_{eff} = 2267 \text{ \AA}$, $\Delta\lambda = 732 \text{ \AA}$) and far-ultraviolet (FUV; $\lambda_{eff} = 1516 \text{ \AA}$, $\Delta\lambda = 268 \text{ \AA}$), respectively. Our UV catalog has been complemented with existing optical and near-infrared photometry. The UV properties of GCs have

¹Department of Astronomy and Space Science, Chungnam National University, Daejeon 305-764, Korea; screy@cnu.ac.kr

²Center for Space Astrophysics, Yonsei University, Seoul 120-749, Korea

³California Institute of Technology, MC 405-47, 1200 East California Boulevard, Pasadena, CA 91125

⁴Department of Physics and Astronomy, University of California, Los Angeles, CA 90095

⁵Korea Astronomy and Space Science Institute, 61-1 Hwaam-dong, Yuseong-gu, Daejeon 305-348, Korea

⁶Center for Astrophysical Sciences, The Johns Hopkins University, 3400 N. Charles St., Baltimore, MD 21218

⁷Observatories of the Carnegie Institution of Washington, 813 Santa Barbara St., Pasadena, CA 91101

⁸Laboratory for Astronomy and Solar Physics, NASA Goddard Space Flight Center, Greenbelt, MD 20771

⁹Department of Astronomy, Columbia University, New York, NY 10027

¹⁰Laboratoire d'Astrophysique de Marseille, BP 8, Traverse du Siphon, 13376 Marseille Cedex 12, France

¹¹Department of Physics and Astronomy, The Johns Hopkins University, Homewood Campus, Baltimore, MD 21218

¹²Space Sciences Laboratory, University of California at Berkeley, 601 Campbell Hall, Berkeley, CA 94720

been analyzed using various combinations of UV–optical and optical–optical colors considered to be tracers of ages and metallicities for simple stellar populations. Comparing M31 data with those of Galactic GCs in the UV with the aid of population models that fully take into account detailed systematic variation of horizontal-branch (HB) morphology with age and metallicity, we find that the age ranges of old GCs in M31 and the Galactic halo are similar. Three metal-rich ($[\text{Fe}/\text{H}] > -1$) GCs in M31 produce significant FUV flux making their FUV– V colors unusually blue for their metallicities. These are thought to be analogs of the two peculiar Galactic GCs NGC 6388 and NGC 6441 with extended blue HB stars. Based on the models incorporating helium enriched subpopulations in addition to the majority of the population that have a normal helium abundance, we suggest that even small fraction of super-helium-rich subpopulations in GCs can reproduce the observed UV bright metal-rich GCs. Young clusters in M31 show distinct UV and optical properties from GCs in Milky Way. In general, young clusters are bluer than old GCs in both NUV and FUV. Population models indicate that their typical age is less than ~ 2 Gyrs and is consistent with the age derived from the most recent high-quality spectroscopic observations. A large fraction of young GCs have the kinematics of the thin, rapidly rotating disk component. However, a subset of the old GCs also shares the thin-disk kinematics of the younger clusters. Most GCs with bulge kinematics show old ages. The existence of young GCs on the outskirts of M31 disk suggests the occurrence of a significant recent star formation in the thin-disk of M31. Old thin-disk GCs may set constraints on the epoch of early formation of the M31 thin-disk. We detect 12 (10) intermediate-age GC candidates in NUV (FUV) identified by previous spectroscopic observations. On the basis of comparing our UV photometry to population models, we suggest that some of spectroscopically identified intermediate-age GCs may not be truly intermediate in age, but rather older GCs that possess developed HB stars which contribute to enhanced UV flux as well as Balmer lines.

Subject headings: galaxies: individual (M31) — galaxies: star clusters — globular clusters: general — ultraviolet: galaxies

1. Introduction

While the principle science goal of the *Galaxy Evolution Explorer* (*GALEX*) has been the study of star formation in the local and intermediate redshift Universe, nearby galaxies

such as M31 have also been surveyed, taking advantage of the wide (1.2 deg) field of view of *GALEX*. Since launch in April 2003, we have been able to image 23 fields near and coincident with M31, now covering nearly all of M31 and its environs. Our first investigation of M31 globular clusters (GCs) using *GALEX* was reported in Rey et al. (2005, hereafter Paper I). The dataset we report on here includes analysis of the coadded images, the wider field, and matching with optical/infrared datasets. While deeper observations of specific regions in M31 will likely occur in the next few years, it is unlikely that the combination of areal coverage and depth will be dramatically superseded by any *GALEX* observations in the next few years.

GCs, as aggregates of coeval stars with small internal dispersion in chemical abundance, are the best examples of simple stellar populations and ideal templates for studying the evolution of stellar populations. Observations of GCs offer the means of clarifying fundamental parameters in various astrophysical processes. At present, GCs are being used to constrain the connection between GC systems and their host galaxies, since they provide tracers of the star formation histories of galaxies in the sense that major star formations in galaxies are concomitant with global GC formation (Brodie & Strader 2006). In this respect, relative ages of GCs within a galaxy or between different galaxies are crucial for understanding the time scale for galaxy formation and subsequent chemical evolution.

The most direct way of measuring age differences among different stellar populations is to compare the observed luminosity levels of the main-sequence turnoffs (MSTOs); for a given metallicity an intrinsically fainter MSTO translates to older ages. Unfortunately this method is limited to the nearest GCs, where individual stars can be resolved and measured well to two magnitudes fainter than the MSTO. Even in the nearest massive spiral galaxy, M31, the MSTO has been reached for only one cluster (G312=B379) and that only after ~ 3.5 days of *HST* ACS integration time (Brown et al. 2004).

Alternatively, ages can be estimated from the horizontal-branch (HB) morphologies of GCs. For a sufficiently old (> 8 Gyr) stellar population, the surface temperature distribution of HB stars is sensitive to age (Lee, Demarque, & Zinn 1994; Yi 2003). Despite uncertainties of the details regarding peculiar HB morphologies in some Galactic GCs (e.g., bimodal HB distribution and extreme HB stars), various studies have suggested that together with metallicity, cluster age is the major parameter controlling the HB morphology (Lee et al. 1994; Sarajedini, Chaboyer, & Demarque 1997; Rey et al. 2001; Salaris & Weiss 2002).

The hot He-burning HB stars and their progenies are most likely the dominant ultraviolet (UV) sources in the nearest old stellar populations (O’Connell 1999; Brown 2004). The integrated far-ultraviolet (FUV) flux depends mainly on the fractional number

of HB stars with T_{eff} hotter than $\sim 10,000$ K, with a modest dependence on their temperature distribution. The production rate of these hot HB stars increases with age. As a result, older GCs are likely to produce stronger FUV flux at a given metallicity (Park & Lee 1997; Yi et al. 1999; Lee, Lee, & Gibson 2002). In this respect, integrated FUV flux can act as an age indicator of GCs (see also Dorman et al. 1995, 2003; Yi 2003; Catelan 2005; Kaviraj et al. 2006). Furthermore, this allows us to investigate mean age distributions of GCs within a single galaxy or among different galaxies, provided that other minor sources of FUV flux (e.g., existence of extreme HB stars due to the helium variation among stellar population in a GC; Lee et al. 2005 and references therein) can be quantified.

The M31 GC system (GCS) is one of the most ideal targets for integrated UV photometry due to its proximity (770 kpc; Freedman & Madore 1990) and populous GCs (more than 300 confirmed GCs; Galleti et al. 2004). Catalogs of M31 GCS are compiled from various imaging observations (Battistini et al. 1980, 1987, 1993; Crampton et al. 1985; Reed, Harris, & Harris 1994; Barmby et al. 2000; Galleti et al. 2004). In addition, many optical spectroscopic observations provide chemical and kinematical properties of M31 GCS (Huchra, Stauffer, & Van Speybroeck 1982; Kent, Huchra, & Stauffer 1989; Huchra, Brodie, & Kent 1991; Brodie & Huchra 1991; Barmby et al. 2000; Perrett et al. 2002). There also have been color-magnitude diagram (CMD) studies of a few M31 GCs using data obtained by *HST* (Ajhar et al. 1996; Fusi Pecci et al. 1996; Rich et al. 1996, 2005; Holland, Fahlman, & Richer 1997; Jablonka et al. 2000; Stephens et al. 2001). All of these studies suggest that the M31 GCS is very similar to that of the Milky Way in many ways. Therefore, the M31 GCs are a kind of bridge between resolved and unresolved stellar populations, making these clusters a critical set of template populations.

On the other hand, there has been growing body of evidence that the GCS of the Milky Way and of M31, the two large spirals in the Local Group, have very different properties and evolutionary histories (c.f. Rich 2004). In contrast to the case of the Milky Way halo GCs with uniformly very old (10 – 12 Gyr) ages, there have been suggestions that the age distribution of M31 GCs is wide. There is a large population of young clusters with ages less than 1 – 2 Gyr and intermediate-age GCs with $\sim 5 - 8$ Gyr (Burstein et al. 2004; Beasley et al. 2004, 2005; Fusi Pecci et al. 2005; Puzia, Perrett, & Bridges 2005) are found in M31. Furthermore, M31 possesses a kinematically distinct group of GCs that follows the disk rotation curve of M31 (Morrison et al. 2004), whereas no such counterparts have yet been discovered in Milky Way. Finally, the nitrogen abundance of the M31 GCs appears to be enhanced relative to that of the Milky Way GCs (Burstein et al. 2004).

To what degree do the GCSs of M31 and the Milky Way share similarities? This question can be answered by taking an approach different from previous studies, i.e. using

UV photometry which is sensitive to age. So far, there has been no systematic UV survey for a large and representative sample of GCs in galaxies, where detailed information on their optical and near-infrared photometry are available. While there are some UV imaging studies of Galactic GCs from satellites such as the *Orbiting Astronomical Observatory (OAO2)*, the *Astronomical Netherlands Satellite (ANS)*, and the *Ultraviolet Imaging Telescope (UIT)* (Dorman, O’Connell, & Rood 1995 and references therein), very little have been carried out for M31 GCs. Using the *International Ultraviolet Explorer (IUE)*, Cacciari et al. (1982) and Cowley & Burstein (1988) obtained the first spectra of a dozen brightest clusters in M31 at low resolution. From rocket-borne UV imaging telescopes, near-ultraviolet (NUV) and FUV fluxes were determined for 17 cluster candidates in M31 (Bohlin et al. 1988). *UIT* observations of M31 detected 43 GCs in NUV but only 4 clusters in the FUV (Bohlin et al. 1993). These studies show that the GCs of M31 and Milky Way cover a similar range of UV–*V* colors. Based on their UV results, Bohlin et al. (1993) suggest that the ages of M31 GCs are as old as the Galactic GCs. However, because the UV sample size of M31 GCs detected from *UIT* is insufficient, especially in FUV which is more sensitive to the age of old stellar populations, the conclusion by Bohlin et al. can not be taken as definitive.

Thanks to the successful launch and operation of *GALEX*, the situation for UV studies of stellar clusters in nearby galaxies has dramatically changed. Using the unprecedented set of *GALEX* photometry of M31 coupled with most recent detailed population models, we are now able to study the global UV characteristics of M31 GCs, and compare them to Milky Way GCs. Using UV images obtained as part of the “*GALEX* Ultraviolet Survey of Globular Clusters in Nearby Galaxies” project, we present the catalog of *GALEX* UV photometry of M31. This catalog is much more homogeneous than the Milky Way UV sample which was collected from several different UV satellites with heterogeneous selection criteria. Unfortunately, *GALEX* cannot study a large fraction of Milky Way and Magellanic clusters because of bright star avoidance restrictions. In this study, we focus on the interpreting the UV photometry of M31 GCs, combining existing optical photometry and corollary data from which we obtain insight into age distributions compared to the Galactic counterparts. In Paper I, we presented our first analysis of *GALEX* photometry of M31 GCs; this study concluded that the UV photometry of the older M31 GC is consistent with no age difference between M31 and the Milky Way. Our current paper supersedes that study both in the accuracy of the photometry and in the numbers of detected M31 GCs.

In Section 2, we describe our observations and data analysis. Section 3 provides a comparison of age distribution of old GCs between M31 and the Milky Way. In Section 4, we report the discovery of UV bright metal-rich GCs in M31, which are thought to be analogs of clusters with peculiar HB morphologies such as NGC 6388 and NGC 6441.

Section 5 describes the young clusters with < 2 Gyr and the age distribution of thin-disk GCs found in M31. In section 6, we discuss the intermediate-age GCs with $4 - 7$ Gyr identified by spectroscopic observations. The conclusions are summarized in Section 7.

2. Observations and Data Analysis

2.1. Observations

The M31 images were obtained as part of the Nearby Galaxy Survey (NGS) carried out by *GALEX* in two UV bands: FUV ($1350 - 1750\text{\AA}$) and NUV ($1750 - 2750\text{\AA}$). The data used in this study consist of images of 23 different 1.25 deg circular fields. Details on the early observations of 14 fields released under the *GALEX Release 1 (GR1)*¹³ can be found in Thilker et al. (2005a) and Paper I. In the interests of increasing both spatial coverage and depth around the M31 field, we have observed an additional nine *GALEX* fields in September – November, 2004, which are included in the *GALEX Release 2 (GR2)*¹⁴. Our strategy for designing the pointings is to cover as wide area as possible around M31, but this was limited by the observing requirements of avoiding extremely UV-bright foreground stars. The resulting coordinates and exposure times of the nine fields are listed in Table 1, and Figure 1 shows the field coverage of each *GALEX* pointing around M31 projected onto $6^\circ \times 6^\circ$ DSS images. Our entire survey coverage of the 23 images is ~ 17 square deg. Photon count maps from single visits were co-added to produce the final image for each field. Preprocessing and calibrations were performed via the *GALEX* pipeline. Details of the *GALEX* instrument and data characteristics are found in Martin et al. (2005) and Morrissey et al. (2005).

2.2. Photometry

In a typical *GALEX* image, point sources within 0.1 deg of the edge appear distorted due to the optics. By examining each image, we decided to only use the inner 1.1 deg field, and pixels outside of this range were masked out prior to doing photometry. Photometry of point sources in the M31 fields were carried out using the DAOPHOT II package (Stetson 1987). For consistency, we have redone photometry for the 14 fields used in Paper I,

¹³<http://galex.stsci.edu/gr1>

¹⁴<http://galex.stsci.edu/gr2>

although we later found that the new photometry is completely consistent with the old results within our errors.

The standard FIND-PHOTOMETRY-PICKPSF-PSF-ALLSTAR routine was applied to each image. We then reran the PHOTOMETRY routine, this time taking outputs from the ALLSTAR program as inputs to ensure that the center of each source is better determined. Visual inspection shows that with this method, centering is much better than solely running the PHOTOMETRY routine, especially for sources in crowded regions. The PHOTOMETRY routine was used to measure fluxes within a radius of 3 pixel ($4''.5$) for each point source in both FUV and NUV images. Aperture corrections were derived using 19 – 44 (5 – 16) isolated stars per frame in NUV (FUV). Mean aperture corrections for the entire data set are -0.248 ± 0.011 and -0.147 ± 0.022 in NUV and FUV, respectively, where errors are standard deviations for the distribution of aperture correction. Finally, flux calibrations were applied to bring all measurements into the AB magnitude system (Oke 1990; Morrissey et al. 2005). Astrometry for images processed through the *GALEX* pipeline is known to be better than $1''.2$ for 80% of the stars in the entire frame (Morrissey, private communication). Our test shows that all stars common in both our photometric catalog and the USNO-B1.0 catalog (Monet et al. 2003) match to within $1''.5$.

2.3. The Ultraviolet Catalog of M31 Globular Clusters

The analysis presented in this work is based on an optically selected sample of GCs and GC candidates extracted from existing catalogs. The most comprehensive catalog of M31 clusters currently available is the Revised Bologna Catalog (RBC; Galleti et al. 2004). This catalog provides positional and photometric information. Out of the total entries in the RBC, we consider 1035 objects consisting of 337 confirmed GCs, 688 GC candidates, and 10 objects with controversial classification. The total number of RBC objects falling in the area covered by our *GALEX* observations is 989.

Sources in our *GALEX* photometry were cross-matched with the RBC objects in the following manner. We decided to use a matching radius of $6''$ considering the combined effect of the astrometry error in RBC ($< 1''$; see Fig 1 of Galleti et al. 2004) and *GALEX* images ($< 1''.2$), and the $4''.6$ FWHM PSF. For each *GALEX* image, we first generate a list of UV-detected RBC sources. We then visually inspect each matched RBC source in each *GALEX* image and reject all spurious sources. Out of the total detected RBC sources, 38% and 44% in each NUV and FUV band were rejected by visual inspections. Finally, we construct a *GALEX* catalog with all UV detected RBC objects.

NUV and FUV magnitudes and their associated errors for each object are listed in Columns (7)–(10) of Table 2. As shown in Figure 1, each *GALEX* image overlaps with at least another image. For objects that lie in these overlapping fields, we have listed their mean magnitudes weighted by their photometric errors. In total, our *GALEX* UV catalog includes 485 and 273 RBC objects in NUV and FUV, respectively. Columns (1) and (2) of Table 2 are identification of M31 GCs adopted from RBC and Barmby et al. (2000), respectively. In column (3), we also add the identification listed in NASA/IPAC Extragalactic Database (NED). Column (4) is the classification flag describing the nature of the entry as listed in RBC; 1: confirmed GCs, 2: candidate clusters, 3: uncertain candidates. RA and DEC coordinates, and *UBVR IJHK* photometry in the table, i.e. columns (5)–(6) and (11)–(18), are also from the RBC. Metallicities ($[\text{Fe}/\text{H}]$) and their errors in columns (19) and (20) are adopted from Barmby et al. (2000), while kinematic residuals in column (21) are taken from Morrison et al. (2004). Figure 2 shows the spatial distribution on the sky of all RBC objects detected in *GALEX* NUV and FUV bands with respect to the M31 disk, NGC 205, and M32.

Extinction correction (including foreground and internal to M31) for each cluster is applied based on a list of $E(B - V)$ kindly provided by P. Barmby. We use the reddening law of Cardelli, Clayton, & Mathis (1989) to estimate the following; $R_{\text{NUV}} = 8.90$ and $R_{\text{FUV}} = 8.16$. In subsequent analyses, we only use confirmed M31 GCs [class 1 in column (4) of Table 2] with $E(B - V) < 0.16$ unless otherwise noted. This limit corresponds to the median value of the $E(B - V)$ distribution for M31 GCs (Barmby et al. 2000).

2.4. *GALEX* UV Detection Rate

We use the B and V magnitudes of RBC to examine the detection rate of clusters in our *GALEX* fields. Figure 3 shows the fraction of RBC objects detected in the NUV and FUV bandpasses as a function of V magnitude and $B - V$ color. Of the 693 objects with both B and V data in RBC, 485 (about 70%) and 273 (about 39%) objects have their entries in the *GALEX* UV catalog for NUV and FUV, respectively (Table 2). The CMD and color histogram show that most of the detected objects belong to an optically blue subgroup with $B - V < 1.2$. It is interesting to note that many of the bluest clusters with $B - V < 0.5$ are detected in the *GALEX* UV bands even though they are fainter than the redder clusters in the optical passband. Most of these blue clusters are young clusters (see Section 5). We estimate that the limiting magnitudes are ~ 22.5 in both NUV and FUV.

2.5. UV–Optical Color Distribution

Figure 4 shows the extinction-corrected $(NUV - V, M_V)$ and $(FUV - V, M_V)$ CMDs for M31 clusters (*large circles*) and Milky Way GCs (*crosses*). The colors and magnitudes of Milky Way GCs were taken from Table 6 of Sohn et al. (2006), and the corrections for difference in effective wavelength of separate observations were made using the same method described in Paper I. A distance modulus of $(m - M)_0 = 24.43$ (Freedman & Madore 1990) was adopted for all M31 clusters. We also plot clusters (*small circles*) with no individual reddening information available in the literature, assuming that they are only affected by the foreground Galactic reddening of $E(B - V) = 0.10$ (Crampton et al. 1985).

The UV-detected M31 clusters essentially cover the entire V -band luminosity range present in the UV-detected sample of Milky Way GCs. The most distinct feature of Fig. 4 is that M31 clusters can be divided into two subgroups based on their UV– V colors; UV-red GCs with $(NUV - V)_0 \gtrsim 3.0$ and $(FUV - V)_0 \gtrsim 4.0$, and UV-blue GCs with $(NUV - V)_0 \lesssim 3.0$ and $(FUV - V)_0 \lesssim 4.0$. The red subgroup of M31 clusters and Milky Way GCs generally occupy the same area in the CMDs. Also, most M31 clusters that belong to the red subgroup have UV– V colors [$(NUV - V)_0 < 4.3$; $(FUV - V)_0 < 5.5$] consistent with theoretically-predicted colors of the UV bright clusters with blue HB morphology (see Section 4). M31 clusters with $(NUV - V)_0 > 4.3$ are likely to have redder HB morphologies and relatively faint UV luminosities.

The blue subgroup of M31 clusters is significantly bluer than the Milky Way GCs. Among their *UIT* sample, Bohlin et al. (1993) also reported clusters much bluer than Milky Way GCs in the NUV. They suggest that these clusters are significantly younger than typical GCs of $> 10Gyr$ (see also Burstein et al. 1984; Bohlin et al. 1988; Cowley & Burstein 1988). Many blue clusters included in our catalog have colors consistent with those [$(NUV - V)_0 \lesssim 2.5$] of younger clusters suggested by Bohlin et al. (1993), while no Galactic counterparts are found. Most of them show stronger fractional UV flux than those of old red GCs, which is suggestive of young ages. We discuss the details of these clusters in Section 5.

3. Age Distribution of Old Globular Clusters

Various studies suggest that UV–optical colors can be an age-dating tool for old stellar systems (Lee et al. 2002; Yi 2003; Paper I; Catelan 2005). Specifically, Lee et al. (2002) and Yi (2003) show that FUV– V color can be more sensitive to ages than any optical-band integrated color. While the strength of FUV flux depends on the fractional

number of hot HB stars, such stars contribute to little light to the optical bands, that are instead dominated by MS and giant stars (Dorman et al. 1995). At a given metallicity, older populations with bluer HB stars should be relatively UV bright, especially in the FUV passband. Thus, the FUV– V color can be a measure of the age variation based on the fraction of the stellar population that appears to be hot HB stars.

Figure 5 shows the $[\text{Fe}/\text{H}]$ vs. $UV-V$ diagrams for M31 clusters (*circles*) and Galactic GCs (*crosses*), as an analog of the $[\text{Fe}/\text{H}]$ vs. HB type diagram of GCs (Lee et al. 1994; as such, bluer colors are now on the right). We restrict the M31 sample to the supposedly old, red clusters with $E(B - V) < 0.16$. The $[\text{Fe}/\text{H}]$ values for M31 is taken from Table 2, while for the Galactic GCs, we adopt the February 2003 version of Harris (1996) catalog¹⁵. While the M31 clusters extend over a wide range of $(NUV - V)_0$ color comparable to that of Galactic GCs, the FUV sample is biased to the blue and metal-poor GCs with no redder $[(FUV - V)_0 > 6.5]$ clusters due to their intrinsically faint FUV brightnesses.

The model isochrones in Fig. 5 are constructed from our evolutionary population models of GCs in the *GALEX* filter system (Chung, Yoon, & Lee 2006, in preparation; see also Lee et al. 2002; Yi 2003). The models include the treatment of the detailed systematic variation of HB morphology with age and metallicity and the fractional contribution of post-asymptotic giant-branch stars. The $\Delta t = 0$ (*solid line*) isochrone corresponds to inner halo Galactic GCs (Galactocentric radius ≤ 8 kpc) of ~ 12 Gyr. The $\Delta t = +2$ Gyr (*long dashed line*) and -2 Gyr (*dotted line*) isochrones are for the models 2 Gyr older and younger than the inner halo Galactic GCs, respectively.

For a given age, HB morphology gets bluer with decreasing metallicity and the population models produce increasing UV flux. As shown in the left panel of Fig. 5, M31 and Galactic GCs follow the general trend indicated by the isochrones. At a fixed metal abundance, the models exhibit rapid blueing of FUV– V colors as the age increases. The large separation among isochrones with different ages (see right panel of Fig. 5) confirms that FUV– V color is more sensitive to ages than any optical-band integrated color. The $NUV-V$ is relatively insensitive to age compared to FUV– V for old ($\gtrsim 8$ Gyr) GCs. This is because not only HB stars but also MSTO stars are responsible for producing integrated NUV flux (Lee et al. 2002; Dorman et al. 2003). The model isochrones fit well the range in color of the GCs and their general locus on the age-metallicity plot. In the right panel of Fig. 5, M31 and Galactic GCs are well located in the age range (± 2 Gyr) of model predictions and show no significant difference in age distribution between the two GCSs. This indicates that M31 and Milky Way GCSs share similarities in mean age and age

¹⁵<http://physwww.mcmaster.ca/%7Eharris/mwgc.dat>

spread, at least, for the old ($\gtrsim 8$ Gyr) GCs.

Many M31 GCs are resolved by *HST* and for those we get HB morphology directly, which makes possible a comparison of the integrated properties of GCs with their actual resolved stellar populations (e.g., Rich et al. 2005). Based on the previous *GALEX* UV data for M31 GCs with known HB morphology from *HST* observations, Paper I confirms that the sensitivity of metallicity and HB morphology to the UV flux is evident in both NUV and FUV bands. Recently, Brown et al. (2004) performed a direct age estimation of the M31 GC B379 by fitting its deep *HST* ACS photometry extending below the MSTO. The extreme stellar crowding caused by the compactness of the cluster results in a less well determined CMD, leading to a somewhat weak age constraint $10_{-1}^{+2.5}$ Gyr. Nonetheless, they suggest that B379 appears to be 2 – 3 Gyr younger than Galactic GCs with similar metallicities. The CMD of B379 shows a tight clump of red HB population consistent with its metallicity and suggested age (Brown et al. 2004; Rich et al. 2005). We detect this cluster (*filled circle*) only in the NUV passband and its $(NUV - V)_0$ color is in good agreement with its HB morphology.

Due to the increased depth of our UV images compared to Paper I, the number of NUV- and FUV-detected GCs with $[Fe/H] > -1$ has grown. It is interesting to note that metal-rich GCs have a wide dispersion of UV colors [$(NUV - V)_0 \sim 4 - 6$] in the $[Fe/H]$ vs. $NUV - V$ plot. Furthermore, although the $NUV - V$ color is relatively less sensitive to the age variation, metal-rich GCs appear to distribute tightly around isochrone of $\Delta t = +2$ Gyr. Since there is no clear evidence that the metal-rich GCs in M31 are systematically older than metal-poor counterparts (e.g., Jiang et al. 2003; Puzia et al. 2005), this feature may reflect the variation of HB morphology and UV flux of M31 metal-rich GCs due to parameters other than metallicity and age (see Sec. 4 for details). Contrary to the case for most Galactic GCs with $[Fe/H] \sim -0.4 - -0.8$, many metal-rich M31 GCs show bluer $NUV - V$ colors (i.e., stronger UV flux). Even some metal-rich GCs show comparable $NUV - V$ colors to those of intermediate metallicity GCs with $[Fe/H] \sim -1 - -1.5$. Only two peculiar metal-rich Galactic GCs, NGC 6388 and NGC 6441 have NUV colors comparable to those of metal-rich M31 GCs. Among the metal-rich M31 GCs, three GCs are also detected in FUV. Most metal-rich GCs detected in NUV are considered to have blue HB stars which contribute flux in NUV passbands, whereas three metal-rich GCs detected in FUV would have more extreme hot blue HB populations (e.g., NGC 6388 and NGC 6441 in the Milky Way; see Sec. 4 for details). In this respect, bright UV flux in M31 metal-rich GCs is in good agreement with the explanation that stronger $H\beta$ lines observed in M31 metal-rich GCs result from the presence of old blue HB stars (Peterson et al. 2003) instead of them being significantly younger than the bulk of M31 GCs (Burstein et al. 1984).

4. UV Bright Metal-Rich Globular Clusters

Galactic GCs such as NGC 1851 and NGC 2808 exhibit bimodal HB distributions, where separate group of hot HB populations coexist with cooler HB components. The most striking cases of GCs with HB bimodalities are NGC 6388 and NGC 6441. These two have pronounced hot HB populations that are not seen in any other Galactic GC of similar metallicity. GCs with $[\text{Fe}/\text{H}] > -0.8$ (e.g. 47 Tuc) are typically faint in the UV due to their HB being dominated by cool stars. Rich, Minniti, & Liebert (1993), however, detected abnormally strong UV flux in NGC 6388 and NGC 6441 from IUE observations. Rich et al. (1993) suggest the existence of hot extreme HB stars in these clusters. The *HST* observations have directly reveal a prominent extended blue HB population, in addition to a well populated red HB sequence (Rich et al. 1997; Piotto et al. 1997). While the cause of peculiar blue HBs in NGC 6388 and NGC 6441 is still not settled, the existence of hot HB stars in metal-rich GCs has implications for understanding the evolution of GCs and, furthermore, elliptical galaxies, since it is related to the origin of UV upturn phenomenon (O’Connell 1999 and references therein).

While NGC 6388 and NGC 6441 stand out as the only two metal-rich GCs with prominent blue HB populations in the Milky Way, it is intriguing to search for examples of extragalactic counterparts to see whether these objects are ubiquitous. UV observations provide an indirect solution for this purpose since integrated UV flux is significantly sensitive to the presence of hot stars in evolved stellar populations. In our previous study (Paper I), we have detected seven clusters with $[\text{Fe}/\text{H}] > -1$ in the NUV but not in the FUV. With our deeper *GALEX* observations, we are now better able to search M31 for counterparts of NGC 6388 and 6441.

Figure 6 is the same as Fig. 5 but now we highlight UV bright metal-rich GCs in M31. In our *GALEX* M31 sample, we find three candidate UV bright metal-rich GCs (*filled circles*: B131, B193, and B225) with $E(B - V) < 0.16$. These have $FUV - V$ colors similar to or smaller than those of NGC 6388 and NGC 6441. Fortunately, CMDs exist for cluster B225 based on images obtained with *HST* WFPC2 (Fusi Pecci et al. 1996; Rich et al. 2005) and NICMOS (Stephens et al. 2001). The BV CMD of B225 (see Fig. 4 of Fusi Pecci et al. 1996; see also Fig. 9 of Rich et al. 2005) show a hint of blue HB population around $(B - V)_o = 0$ in addition to the red HB population. Overall, the HB morphology appears to be similar to those of NGC 6388 and NGC 6441, although the existence of an extended blue HB sequence in B225 is difficult to confirm because the CMD reach only 1 mag fainter than the HB level. The $[\text{Fe}/\text{H}]$ values determined from the photometry by Fusi Pecci et al. (1996) and Rich et al. (2005) are also similar to those for NGC 6388 and NGC 6441. Deep imaging with *HST* is required to judge whether the UV bright metal-rich clusters

(including B225) are M31 counterparts of NGC 6388 and 6441.

Using the Ca II index as an indicator of HB morphology (Rose 1984, 1985), Beasley et al. (2005) suggest that two M31 GCs (B158 and B234) are candidate metal-rich GCs that may have blue HB components and therefore are analogs of NGC 6388 and NGC 6441. The Ca II indices of these two M31 GCs are similar to those of NGC 6388 and NGC 6441 and are systematically smaller than those of other M31 and Galactic GCs with similar metallicity (see Fig. 19 of Beasley et al. 2005). We detected B158 ($[\text{Fe}/\text{H}] = -1.08$) in both NUV and FUV, but B234 ($[\text{Fe}/\text{H}] = -0.84$) is detected only in NUV (*filled triangles* in Fig. 6). As shown in Fig. 6, cluster B234 shows rather larger NUV flux than those of NGC 6388 and NGC 6441. On the other hand, cluster B158 shows normal UV colors in both NUV and FUV which are consistent with its relatively low metallicity.

In Fig. 6, we include the extremely massive and moderately metal-rich ($[\text{Fe}/\text{H}] = -1.08$; Barmby et al. 2000) M31 GC G1 (*filled square*). The CMD of G1, as presented by Rich et al. (2005), is similar to that of 47 Tuc; the HB is dominated by cool stars. However, G1 shows a notable minority population of blue HB stars near the detection limit, which is consistent with slightly stronger UV flux than GCs with similar metallicity (see also Peterson et al. 2003). Therefore, G1 is considered to be a moderate metal-rich GC with low-level enhancement of UV flux.

According to its HB morphology in the *HST* CMD, cluster B225 is almost certainly an old GC. However, since young populations can also contribute to the integrated UV flux (see also Sec. 5), we need to check if the other two clusters B131 and B193 are similarly old. In Fig. 6, we superpose a 1 Gyr isochrone (*short dashed line*) in addition to three isochrones of age 10 – 14 Gyr. The UV bright metal-rich clusters in M31 and NGC 6388/NGC 6441 sit well between the 1 and 14 Gyr isochrones making the age discrimination ambiguous. However, using the color-color diagram such as $B - V$ vs. $FUV - V$ as shown in Figure 7, it is possible to separate young clusters from old GCs. For example, young clusters are bluer than old GCs in both $B - V$ and $FUV - V$ for the metallicity range of $[\text{Fe}/\text{H}] < -1.0$. Metal-rich ($[\text{Fe}/\text{H}] > -1.0$) young GCs in the range of $(FUV - V)_o > 4.0$ are also reasonably deviated from the old GCs. All candidate UV bright metal-rich GCs in M31 follow the isochrones for old ages, which confirm that they are bona-fide old metal-rich GCs with strong FUV flux.

Recently, Sohn et al. (2006) obtained *HST* STIS FUV and NUV photometry of 66 GCs in the giant elliptical galaxy M87. A remarkable and unanticipated result is that M87 GCs have distinct UV properties from GCs in the Milky Way and M31, despite strong overlap in optical properties. Their $FUV - V$ colors are up to 1 mag bluer than any Milky Way GC. M87 GCs appear to produce larger hot HB populations and therefore much more

UV flux than do Milky Way and M31 counterparts at a given metallicity. However, there is no ready explanation for the prominent strength of hot HB stars in the M87 GCs (see Sohn et al. 2006 for details). In $[\text{Fe}/\text{H}]$ vs. $UV-V$ diagrams of Figure 8, we compare GCs in M87 (*filled squares*; Sohn et al. 2006) with those in Milky Way (*crosses*) and M31 (*open circles*). We convert magnitudes of M87 GC data in STMAG system to those of the *GALEX* filter system. The $[\text{Fe}/\text{H}]$ values of M87 GCs are transformed from $V-I$ (Sohn et al. 2006). Most M87 GCs are systematically brighter in UV than the Milky Way and M31 GCs at any given $[\text{Fe}/\text{H}]$. However, it is worth noting that the distributions of UV bright metal-rich GCs in M31 (*filled circles*) and NGC 6388 and NGC 6441 are in good agreement with that of metal-rich M87 GCs in $[\text{Fe}/\text{H}]$ vs. $(FUV-V)_0$ diagram. This indicates that the UV-detected GCs in M87 may be mostly analogs of NGC 6388 and NGC 6441. The UV bright metal-rich GCs in M31 and Milky Way constitute a distinct type of stellar population and share their properties with metal-rich GCs in M87. The inference is that these anomalous UV bright metal-rich GCs may be ubiquitous in more or most galaxies, although M87 is distinct from the other two.

While we still lack a definitive explanation, several scenarios have been suggested to elucidate the observed peculiar HB morphology and RR Lyrae periods in the NGC 6388 and NGC 6441 (see Catelan 2005 for details and references therein). A recently revived possibility is that helium abundance may play an important role for the existence of the hot extreme HB stars and for pronounced UV flux of metal-rich GCs. S.-J. Yoon et al. (2006, in preparation) discuss the possibility that the bimodal nature of the HBs of NGC 6388 and NGC 6441 can be attributed to a small fraction of super-helium-rich ($Y \sim 0.3$) population due to the self-helium-enrichment (see also Catelan 2005; Moehler & Sweigart 2006). Considering the CMD morphologies and the RR Lyrae properties, they conclude that the stellar population simulations based on the super-helium rich hypothesis reproduce the observations more successfully for these GCs. Meanwhile, it is also proposed that the subpopulations of two other Galactic GCs, ω Centauri and NGC 2808, are super-helium-rich (D’Antona & Caloi 2004; Lee et al. 2005; D’Antona et al. 2005; Bekki & Norris 2006). In the case of ω Cen, the helium rich population actually occupies a distinct main sequence locus. Furthermore, combining *HST* STIS (Sohn et al. 2006) and WFPC2 (Jordan et al. 2002) photometry with stellar population models, S. Kaviraj et al. (2006, in preparation) propose that the majority of UV-bright M87 GCs show strong signatures of minor super-helium-rich populations. All of these results suggests that the HB morphology is also governed by the helium abundance variation among the stellar populations in some GCs as a possible third parameter.

Figure 9 is a comparison of UV bright metal-rich GCs in Milky Way (NGC 6388 and NGC 6441), M31 (*filled circles*), and M87 (*filled squares*) with our model isochrones

overlaid. Dotted lines are for the case in which all the GCs have same primordial helium abundance of $Y = 0.23$ but different ages. Dashed lines are for the case with minority population of helium enhancement ($Y = 0.33$) in addition to the majority of the population with normal helium abundance ($Y = 0.23$) within a model GC at the same age of 12 Gyr. These correspond to models that include the extreme HB stars with $T_{eff} > 15,000$ K due to the helium enhancement (see Lee et al. 2005; D’Antona et al. 2005). Different model lines with high helium abundances indicate different population number fraction of helium enhancement (left to right, 10%, 20%, 30%, and 50%) within a GC. Strong UV flux can be reproduced by even small fraction of helium enhanced subpopulation within a GC. A reasonable agreement between observed UV colors of UV bright metal-rich GCs and models is obtained when we adopt a wide range of helium abundance. One of the possibilities for the strong UV flux in metal-rich GCs may be understood as being due to the contribution of extreme hot HB stars in these clusters as a consequence of the large differences in helium abundances that easily overcomes the metallicity effect.

5. Young and Thin-Disk Globular Clusters

5.1. Young Globular Clusters

Young star clusters with mass range $10^4 - 10^6 M_{\odot}$ has been identified in a few distant galaxies including Local Group members (Larsen & Richtler 1999). Observations for such objects may provide valuable information concerning the formation and evolution of old GCs in galaxies. M31 is not exception in having these kinds of clusters that have similar luminosity and structure as the Milky Way old GCs, but show significantly bluer $[(B - V)_0 < 0.45]$; Fusi Pecci et al. 2005] integrated optical colors. Interestingly, in the Local Group, the Milky Way appears to be the large galaxy that lacks such young massive compact clusters. There are some fragmentary studies of young clusters in M31 (Fusi Pecci et al. 2005 and references therein). Early studies report the existence of these blue clusters in M31 (Vetevnik 1962; van den Bergh 1967, 1969; Searle 1978), and recent studies have concentrated on the properties of these objects (Williams & Hodge 2001a,b; Beasley et al. 2004; Burstein et al. 2004; Puzia et al. 2005; Fusi Pecci et al. 2005).

In the context of understanding the spectral evolution of simple stellar populations of star cluster, the integrated spectrum of young cluster is dominated by short-lived, young massive stars with strong UV flux (see Fig. 9 of Bruzual and Charlot 2003). Therefore, compared to the optical passband, the UV is a good probe to identify young clusters. In previous UV observations using rocket-borne telescope and *UIT*, only a handful of young GC candidates in M31 were identified (Bohlin et al. 1988, 1993). Based on their blue UV

colors, Bohlin et al. suggested that these are clusters with ages less than 1 Gyr that may be analogous to the large populations of “blue globulars” in LMC.

The combination of the UV– V color with the $B - V$ color clearly improves the discrimination between old and young GCs. This is based on a comparison of the slope of the spectral energy distribution in the $B - V$ range with the slope from the UV to V band with distinctly different ages (Yi 2003). Figure 10 shows $B - V$ vs. UV– V diagrams for young GCs (B210, B222, B315, B321, B322, B327, B484, and V031; *filled circles*) found from the recent high-quality spectroscopic observations (Beasley et al. 2004; Burstein et al. 2004), compared with the old GCs (*open circles*). Among the young GCs in the list of Beasley et al. (2004), we exclude the slightly older ($\sim 2 - 3$ Gyr) metal-poor cluster B292. The mean distribution of young GCs is biased to bluer colors in both optical and UV colors. Especially, in the right panel of Figure 10, young GCs are clearly separated from the old GCs. Since the reddening values of these young GCs are not available from Barmby et al. (2000), we adopt the mean foreground reddening value of M31 field, $E(B - V) = 0.10$. Ages of these young GCs are estimated to be in the range 0.5 Gyr (*long dashed line*) – 1 Gyr (*solid line*) according to our population models, which are consistent with results of Beasley et al. (2004) and Williams & Hodge (2001a).

One caveat for the studies of young GCs is that some of the suggested very young GCs in distant spiral galaxies may be spurious identifications rather than bona-fide clusters. Most recently, from their high spatial resolution observations with Keck laser-guide star adaptive optics system, Cohen et al. (2005) found that a large fraction of the putative very young (< 2 Gyr) GCs in M31 may not be genuine GCs, but probably asterisms. If this is true, unless we undertake a similar survey for asterisms and identify true young GCs, we could not provide the exact frequency of young GCs, which is important to constrain the formation rate of GCs. Four objects (B223, B216, B314, and B380; *filled triangles*) identified as asterisms by Cohen et al. (2005) are found in our UV catalog. They are also included in the list of young GCs of Beasley et al. (2004) and Burstein et al. (2004). As shown in Fig. 10, these objects have similar optical/UV colors to those of other possible young GCs; the UV photometry cannot be used to distinguish true clusters from asterisms.

Meanwhile, Williams & Hodge (2001a) presented *HST* images for four young genuine M31 GCs that have the appearances of typical GCs (see Fig. 1 of Fusi Pecci et al. 2005). CMDs with resolved stellar populations of these clusters yield ages less than 200 Myr. Four young GCs (B315, B319, B342, and B368; *open squares* in Figure 10) of Williams & Hodge (2001a) are identified in both NUV and FUV passbands. Although Williams & Hodge (2001a) estimated $E(B - V)$ values of these clusters using the color of the upper MS stars of CMDs, we adopt $E(B - V) = 0.10$ as their reddening values for consistency.

The B and V magnitudes are from the Table 1 of Williams & Hodge (2001a). Their UV colors are fully consistent with those of model predictions with young ages. The integrated luminosities and half-light radii of these clusters indicate that they are more massive and compact than counterparts in Milky Way. Furthermore, their luminosities are quite similar to young clusters found in many other spiral galaxies (Larsen & Richtler 1999; Larsen 2004). Evidently, these massive and compact young clusters are common in galaxies and/or, at least, in the Magellanic Clouds and M31; in more distant galaxies, the problem of confusion with individual stars and clusters will be a more significant issue, however.

5.2. Thin-Disk Globular Clusters

In addition to the detection of many young GCs in M31 from various observations, Morrison et al. (2004) argues for the presence of a subsystem of GCs in M31 with thin-disk kinematics, based on the spectroscopic data of Perrett et al. (2002). Thin-disk GCs are identified as clusters with residual radial velocity (δ) less than 0.75 km s^{-1} (see Morrison et al. 2004 for details). This new population of GCs is found across the entire disk of M31 and has a wide range of metallicities ranging from $[\text{Fe}/\text{H}] < -2.0$ to above solar, indistinguishable from M31 GC population. Lacking a direct measurement of the ages of these GCs, Morrison et al. (2004) speculate that M31 had a relatively large thin-disk during its early evolution, because these clusters appear to be old and metal-poor. Furthermore, they suggest that the existence of such a disk with cold kinematics is not attributable to a substantial merger event or significant perturbation since the clusters were formed. This is in contrast to the suggestion that M31 was formed by an equal-mass merger 6 – 8 Gyr ago (e.g., Brown et al. 2003).

Subsequent studies of the disk clusters (Burstein et al. 2004; Beasley et al. 2004; Puzia et al. 2005) have reported that some thin-disk GC samples of Morrison et al. (2004) are massive young GCs. The recent extensive study by Fusi Pecci et al. (2005) found a population of 67 massive blue clusters in the disk of M31. These clusters have very blue colors and enhanced $\text{H}\beta$ absorption lines indicating an age of ~ 2 Gyr, and possess kinematics similar to that of the M31 thin-disk. Fusi Pecci et al. (2005) confirmed that these massive blue thin-disk clusters appear to avoid the inner regions of the M31, but are rather well projected onto the outer disk and coincide with continuous star-forming regions in the spiral arms. These results lead to the suspicion that a significant population of old metal-poor clusters exists in the thin-disk of M31 as suggested by Morrison et al. (2004).

In order to constrain the formation epoch and evolution of the M31 thin-disk and the clusters in it, further studies of the age distribution with larger sample of thin-disk GCs

are required. Specifically, it is crucial to explore among clusters with thin-disk kinematics, (1) the number of young clusters and (2) whether there exists any old GC. At the same time, it is also useful to compare the age distribution of thin-disk GCs with that of GCs not showing thin-disk kinematics (i.e, bulge GCs). For these purposes, we use *GALEX* UV data of M31 GCs to investigate the age distribution of subgroups of GCs with different kinematic properties.

Figure 11 shows the $B - V$ vs. $UV - V$ color-color diagrams for M31 GCs with thin-disk kinematics (*filled circles*). As suggested by Morrison et al. (2004), GCs with absolute residual radial velocity less than 0.75 km s^{-1} are selected as thin-disk GCs. The dashed horizontal line corresponds to a reference color value [i.e., $(B - V)_o = 0.45$] for selecting young clusters following Fusi Pecci et al. (2005). Their locations are consistent with those of confirmed young clusters (Figure 10) and our population models with less than 1 Gyr. It is evident that most candidate young GCs with blue optical colors [$(B - V)_0 < 0.45$] show thin-disk kinematics. At least, about 70% of young GC sample with $(B - V)_0 < 0.45$ detected in FUV falls into the thin-disk subsystem.

Besides GCs with known kinematic information from Morrison et al. (2004), some blue GCs without kinematic data [open circles with $(B - V)_0 < 0.45$] also show young ages. According to the age distribution of GCs with bulge kinematics (see Figure 12), they may be also possible thin-disk young GCs, but radial velocity measurements for these clusters are needed.

It is worth noting that among old red GCs with $(B - V)_0 > 0.45$, some thin-disk GCs are also found, although their fraction is not large. This indicates that thin-disk GCs display large age spread, which is in good agreement with the results of Puzia et al. (2005). In turn, this suggests that the M31 thin-disk and clusters following its kinematics are formed at the early formation stage of M31, and that later on, a significant number of clusters are formed in the disk of M31.

For comparison, in Figure 12, we plot M31 GCs with bulge kinematics (*filled circles*) which are selected from the Morrison’s δ larger than 0.75 km s^{-1} . Contrary to the thin-disk GCs, the most striking feature is that they are biased to the relatively red optical and UV colors. This indicates that GCs with bulge kinematics, in the mean, belong to the old subsystem.

In Figure 13, we compare the distribution of M31 thin-disk GCs (*filled circles*) with that of bulge GCs (*filled squares*). We divide thin-disk GCs into two groups: blue [$(B - V)_0 < 0.45$; *large filled circles*] and red [$(B - V)_0 > 0.45$; *small filled circles*] GCs. Since [Fe/H] values of Barmby et al. are not available for many thin-disk GCs of Morrison et al. (2004),

we instead adopt $[\text{Fe}/\text{H}]$ from Perrett et al (2002). In addition to the model isochrones with old ages comparable to mean Galactic halo (10 – 14 Gyr, *dotted lines*), we also superpose our young isochrones with 1 Gyr (*solid line*) and 0.5 Gyr (*long dashed line*). Optically blue thin-disk GCs show systematically stronger UV flux than do red thin-disk GCs at a given metallicity. This again confirms that the majority of blue thin-disk GCs are young with ages less than ~ 1 Gyr. GCs with bulge kinematics are biased to the red UV color distribution, which is an indication of their old ages.

Besides the age distribution, the metallicity of young thin-disk GCs is another important clue to understand the formation and evolution of the thin-disk of M31. In Fig. 13, the UV bright and young thin-disk GCs appear to be systematically more metal-poor than their old counterparts. Morrison et al. (2004) speculate that the large disk of M31 had been in place at early epoch based on the existence of metal-poor thin-disk GCs in the catalog of Perrett et al. (2002). However, Fusi Pecci et al. (2005) claim that there may be a systematic bias in $[\text{Fe}/\text{H}]$ determination for young GCs by Perrett et al. (2002) due to the age-metallicity degeneracy effect. Fusi Pecci et al. (2005) suggest that these young GCs may be possibly more metal-rich by ~ 1 dex in $[\text{Fe}/\text{H}]$. Other hints of high metallicity for young thin-disk GCs supports this possibility (e.g., Williams & Hodge 2001a; Beasley et al. 2004). If this is the case, the metallicity of young GCs are similar or slightly larger than that of old GCs. More spectroscopic observations of M31 young thin-disk GCs are required to clarify this issue.

6. Intermediate-Age Globular Clusters

Spectroscopic and spectrophotometric observations of M31 clusters support the existence of intermediate-age GCs with mean age ~ 5 Gyr (Jiang et al. 2003; Burstein et al. 2004; Beasley et al. 2005; Puzia et al. 2005). However, the age dating of extragalactic GCs via line index measurements is affected by (1) uncertainties in spectroscopic observations and (2) the degeneracy between age and HB morphology on the strength of Balmer lines (e.g., de Freitas Pacheco & Barbuy 1995; Lee et al. 2000; Maraston et al. 2003; Thomas, Maraston, & Bender 2003; Schiavon et al. 2004; Trager et al. 2005). While stars near the MSTO region are the most dominant sources for the integrated strength of Balmer lines, blue HB stars also make a substantial contribution to the equivalent widths of these lines. Enhancement of Balmer lines due to these He burning stars are maximized when the distribution of HB stars is centered at $(B - V)_0 \sim 0$ or $T_{eff} \sim 9500\text{K}$. The effect of old blue HB stars on the strong Balmer lines is such that the spectroscopic ages are significantly underestimated when such populations are present in GCs.

In this respect, $FUV - V$ colors provide a useful tool for discriminating the intermediate-age subpopulation from old (> 10 Gyr) and young (< 1 Gyr) GCs within a wide range of metallicity. While old and young GCs show significantly large FUV to optical flux ratios, the intermediate-age GCs are relatively faint in FUV (see Fig. 2 of Lee, Lee, & Gibson 2003). This is because intermediate-age GCs only contain warm MSTO stars which are not hot enough to produce a significant amount of FUV flux. If these are truly intermediate-age objects as suggested by spectroscopic observations, then they should not be detected (or be very faint) in our *GALEX* FUV photometry within the detection limit (Lee & Worthey 2005).

Puzia et al. (2005) derived spectroscopic ages for 70 GCs in M31 based on Lick index measurements. They find a population of intermediate-age GCs with ages 5 – 8 Gyrs and a mean metallicity of $[Z/H] \sim -0.6$. Independently, Burstein et al. (2004) and Beasley et al. (2005) also find two and six intermediate-age GCs in M31, respectively. Here, we consider 12 intermediate-age GCs with spectroscopically derived ages of 4 – 7 Gyr from Table A.3 of Puzia et al. (2005). There are four intermediate-age clusters in common between Beasley et al. (2005) and Puzia et al. (2005). Most of the intermediate-age candidates have metallicities in the range $[Fe/H] < -1.0$ (Barmby et al. 2000). Among the 16 intermediate-age candidates identified by Puzia et al. (2005), Beasley et al. (2005), and Burstein et al. (2004), 12 and 10 GCs¹⁶ are detected in *GALEX* NUV and FUV passband, respectively.

In Figure 14, we show $(B - V)_0$ vs. $(FUV - V)_0$ color-color diagram for the intermediate-age GC candidates (*filled circles*) detected in FUV, regardless of their $E(B - V)$ values. For comparison, we also plot old M31 (*open circles*) and Milky Way (*crosses*) GCs. The model isochrones in Fig. 14 are for old (10, 12, and 14 Gyr; *dotted lines*), intermediate (5 Gyr; *solid line*), and young (1 Gyr; *long dashed line*) ages. The most striking feature of Fig. 14 is that all but one (B126) of the intermediate-age GC candidates detected in FUV are placed in the color-color diagram generally occupied by old GCs of age $\sim 12 - 14$ Gyr. This suggests that most, if not all, of these intermediate-age GC candidates are in fact as old as the oldest M31 GCs. In this regard, it is important to note that intermediate-age cluster candidates B311 (Bursten et al. 2004) and B058 (Puzia et al. 2005) show clearly developed blue HBs in recent *HST* CMDs by Rich et al. (2005). Individual CMDs for other intermediate-age GCs will give definitive answers to how the Balmer lines are affected by the presence of blue HB populations.

¹⁶Namely, they are B058, B110, B178, B182, B185 (NUV only), B126, B232, B292, B311, B337, B365, and NB67 (NUV only). Four intermediate-age candidates (B301, NB16, NB81, and NB89) are not detected in both NUV and FUV.

7. Summary and Conclusions

We present the *GALEX* NUV and FUV photometry for GCs in M31 based on a mosaic of observations covering the whole of M31. By cross-matching with objects in the RBC catalog, we detected 485 and 273 GCs in NUV and FUV, respectively, which are the most complete and homogeneous UV data for M31 GCs. We present our final UV catalog of M31 GCs, which is complemented with optical and near-infrared photometry for all UV-detected GCs.

We find that UV–optical color plays an important role as an age indicator while other possible contamination should be carefully considered (e.g., existence of extreme HB stars due to the helium variation among stellar populations in a GC; Lee et al. 2005 and references therein). At a given metallicity, the older populations with bluer HB stars are relatively UV bright, especially in the FUV passband. Comparing M31 data with Galactic GCs in the UV based on our population models that include the treatment of the detailed systematic variation of HB morphology with age and metallicity, we find that the age ranges of old GCs in M31 and Galactic halo are similar. While deep HST imaging of field populations in M31 find that disparate distant fields all show substantial 6-10 Gyr age ranges with only a minority of old stars (Brown et al. 2006) our UV study of the GCS continues to confirm the view that the GCS of M31 is old and similar to that of the Milky Way, except for a minority of either very young or intermediate-age clusters. The *GALEX* mission will rapidly enlarge the sample of GCs in nearby galaxies within 3 – 4 Mpc and enable us to quantify any systematic mean age differences between cluster systems, modulo issues such as the effect of minority helium enriched populations.

Metal-rich GCs have a hint of wide dispersion of NUV colors, which reflects the variation of HB morphology and UV flux of metal-rich GCs in M31 due to parameters other than metallicity and age. Furthermore, while most metal-rich GCs are faint in the FUV, we find three candidate metal-rich ($[\text{Fe}/\text{H}] > -1$) GCs with significant FUV flux like that found for the peculiar Galactic GCs, NGC 6388 and NGC 6441, with extended blue HB stars. This indicates that even metal-rich M31 GCs may have hot blue HB populations rivaling any metal-poor GCs. Our discovery demonstrates for the first time that a possible population of hot extreme HB stars can exist in old, metal-rich GCs in M31. The UV properties of UV bright metal-rich GCs in M31 and Milky Way are in good agreement with those of metal-rich GCs in M87, which suggests that these anomalous UV bright metal-rich GCs may be ubiquitous in many galaxies. In this regard, deep *HST* ACS FUV observations (PID #10901) for GCS of NGC 1399 will provide an opportunity to determine whether GCs in NGC 1399 also share characteristics with those in M87 (and with UV bright metal-rich GCs in Milky Way and M31).

According to our population models, the strong UV flux of UV bright metal-rich GCs can be reproduced by even a small fraction of helium enhanced subpopulation in addition to the majority of the population having normal helium abundance within a GC. We suggest that a reasonable agreement between observed UV colors of UV bright metal-rich GCs and population models can be achieved when we adopt a wide range of helium abundance. The discovery of UV bright metal-rich GCs is important in the context that the very hot extreme HB stars may be responsible for the upturn in FUV flux seen in luminous metal-rich elliptical galaxies and spiral bulges.

We confirm that the subsystem of blue GCs in M31 with thin-disk kinematics consists of dominantly young (< 1 Gyr) GCs. This is in line with the suggestion that significant formation of possible massive clusters was triggered recent epoch in the disk of M31. We also find a thin-disk subset among red GCs in M31 and their ages are likely old (> 10 Gyr). Based on our results from *GALEX* UV observations and previous studies of M31 GCs (Fusi Pecci et al. 2005; Puzia et al. 2005), we suggest that the overall feature of M31 thin-disk GCs regarding their formation and evolution is as follows: a small fraction of GCs (i.e., red thin-disk GCs) belonging to the thin-disk are formed at an early epoch and maintain their kinematic properties. Significant formation of a large fraction of GCs (e.g. blue thin-disk GCs) appears to have occurred recently (< 1 Gyr) in the thin-disk of M31. This leads us to conclude that the M31 and Milky Way GCSs are even more different than had previously been suggested.

It is intriguing to note that the formation regions of young thin-disk GCs (e.g., Morrison et al. 2004) coincide with those of massive star formation in the outskirts of M31 observed by *GALEX* (Thilker et al. 2005a) and *Spitzer* (Gordon et al. 2006). This is also consistent with the most recent results of *GALEX* observations that some nearby spiral galaxies (M33, M51, M83, and M101, Bianchi et al. 2005; Thilker et al. 2005a, b) show similar galactocentric gradients of $FUV - NUV$ color becoming bluer outward, which indicates younger stellar populations toward the outer parts of the galaxy disk. While it may be tempting to consider a connection between young thin-disk GCs and the recently discovered extended disklike stellar structure around the M31 (Ibata et al. 2005), the age distribution of the M31 disk population at 30 kpc is still dominated by 4-10 Gyr old stars (Brown et al. 2006).

The discovery of young GC-like objects in the disk of M31 provides an opportunity to study the ongoing process of GC formation at the current epoch and to connect with the properties of old GCs (Larsen 2004). While many observational results establish the presence of young massive clusters in a variety of environments that are peculiar in some ways (e.g., starburst galaxies and merger galaxies), the existence of young GCs in M31 disk

may be evidence that young massive clusters can form even in the disks of normal spiral galaxies (see the recent review of Larsen 2004 and references therein). In this respect, it is important to extend our UV studies of GCS to other galaxies such as M33, LMC/SMC, and Cen A. Such studies are currently underway and the results will be presented in our forthcoming papers.

We detect 12 and 10 intermediate-age GC candidates classified by previous spectroscopic observations in NUV and FUV, respectively. On the basis of the UV photometry, we cautiously suggest that some of the spectroscopically identified-age GCs may not be truly intermediate-age objects, but rather older GCs with developed HB stars that contribute to enhanced UV flux as well as Balmer lines. We suggest that the FUV photometry can be an indirect indication of the presence of intermediate-age GCs and may provide a complementary test of the spectroscopic observations for the age dating of GCs. Since spectroscopic results and UV photometry are based on the integrated properties of stellar population, deep *HST* imaging with high spatial resolution for intermediate-age GC candidates is critical in order to derive their HB morphologies. In this respect, the outcomes of the *HST* ACS observations (PID #10631) of intermediate-age GC candidates (B337, B336, B058, B049, B206D, B292, and B350) of M31 are highly anticipated. This will provide a definite answer to the question of whether spectroscopically derived ages for intermediate-age GCs are due to the truly younger ages or the anomalous hot HB stars. In any case, our *GALEX* UV photometry of the intermediate-age GC candidates will have important implications for spectroscopically derived age and metallicities of clusters in distant stellar populations.

We are grateful for the clarifications and improvements suggested by an anonymous referee. *GALEX* (Galaxy Evolution Explorer) is a NASA Small Explorer, launched in April 2003. We gratefully acknowledge NASA's support for construction, operation, and science analysis for the *GALEX* mission, developed in cooperation with the Centre National d'Etudes Spatiales of France and the Korean Ministry of Science and Technology. Yonsei University participation was supported by the Creative Research Initiative Program of MOST/KOSEF, for which we are grateful. This work was supported by the Korea Research Foundation Grant funded by the Korean Government (MOEHRD) (KRF-2005-202-C00158).

REFERENCES

- Ajhar, E. A., et al. 1996, *AJ*, 111, 1110
- Barmby, P., Huchra, J. P. Brodie, J. P., Forbes, D. A., Schroder, L. L. & Grillmair, C. J. 2000 *AJ*, 119, 727
- Battistini, P., Bonoli, F., Braccesi, A., Fusi-Pecchi, F., Malagnini, M. L., & Marano, B. 1980, *A&AS*, 42, 357
- Battistini, P., Bonoli, F., Braccesi, A., Federici, L., Fusi Pecci, F., Marano, B., Borngen, F. 1987, *A&AS*, 67, 447
- Battistini, P., Bonoli, F., Casavecchia, M., Ciotti, L., Federici, L., Fusi-Pecchi, F. 1993, *A&A*, 272, 77
- Beasley, M. A., Brodie, J. P., Strader, J., et al. 2004, *AJ*, 128, 1623
- Beasley, M. A., Brodie, J. P., Strader, J., et al. 2005, *AJ*, 129, 1412
- Bekki, K., & Norris, J. E. 2006, *ApJ*, 637, L109
- Bianchi. L., et al. 2005, *ApJ*, 619, L71
- Bohlin, R. C., Cornett, R. H., Hill, J. K., Hill, R. S., & Stecher, T. P. 1988, *ApJ*, 334, 657
- Bohlin, R. C., Deutsch, E. W., McQuade, K. A., et al. 1993, *ApJ*, 417, 127
- Brodie, J. P., & Huchra, J. 1991, *ApJ*, 379, 157
- Brodie, J. P., & Strader, J. 2006, preprint (astro-ph/0602601)
- Brown, T. M. 2004, *Ap&SS*, 291, 215
- Brown, T. M., Ferguson, H. C., Smith, E., Kimble, R. A., Sweigart, A. V., Renzini, A., Rich, R. M., & VandenBerg, D. A. 2003, *ApJ*, 592, L17
- Brown, T. M., Ferguson, H. C., Smith, E., Kimble, R. A., Sweigart, A. V., Renzini, A., Rich, R. M., & VandenBerg, D. A. 2004, *AJ*, 127, 2738
- Brown, T. M., Smith, E., Ferguson, H. C., Rich, R. M., Guhathakurta, P. G., Renzini, A., Sweigart, A. V., & Kimble, R. A. 2006, *ApJ*, in press
- Bruzual, G., & Charlot, S. 2003, *MNRAS*, 344, 1000
- Burstein, D., Faber, S. M., Gaskell, S. M., & Krumm, N. 1984, *ApJ*, 287, 586
- Burstein, D., Li, Y., Freeman, K. C., et al. 2004, *ApJ*, 614, 158
- Cacciari, C., Cassatella, A., Bianchi, L., Fusi Pecci, F., & Kron, R. G. 1982, *ApJ*, 261, 77
- Cardelli, J. A., Clayton, G. C., & Mathis, J. S. 1989, *ApJ*, 345, 245
- Catelan, M. 2005, preprint (astro-ph/0507464)

- Cohen, J. G., Matthews, K., & Cameron, P. B. 2005, *ApJ*, 634, L45
- Cowley, A. P., & Burstein, D. 1988, *AJ*, 95, 1071
- Crampton, D., Cowley, A. P., Schade, D., & Chayer, P. 1985, *ApJ*, 288, 494
- D’Antona, F., & Caloi, V. 2004, *ApJ*, 611, 871
- D’Antona, F., Bellazzini, M., Caloi, V., Fusi Pecci, F., Galleti, S., & Rood, R. T. 2005, *ApJ*, 631, 868
- de Boer, K. 1982, *A&AS*, 50, 247
- de Freitas Pacheco, J. A., & Barbuy, B. 1995, *A&A*, 302, 718
- Dorman, B., O’Connell, R. W., & Rood, R. T. 1995, *ApJ*, 442, 105
- Dorman, B., O’Connell, R. W., & Rood, R. T. 2003, *ApJ*, 591, 878
- Freedman, W. L., & Madore, B. F. 1990, *ApJ*, 365, 186
- Freitas Pacheco, J. A., & Barbuy, B. 1995, *A&A*, 302, 718
- Fusi Pecci, F., et al. 1996, *AJ*, 112, 1461
- Fusi Pecci, F., Bellazzini, M., Buzzoni, E., et al. 2005, *AJ*, 130, 554
- Galleti, S., Federici, L., Bellazzini, M., Fusi Pecci, F., & Macrina, S. 2004, *A&A*, 416, 917
- Gordon, K. D., et al. 2006, *ApJ*, 638, L87
- Harris, W. E. 1996, *AJ*, 112, 1487
- Holland, S., Fahlman, G. G., & Richer, H. B. 1997, *AJ*, 114, 1488
- Huchra, J., Stauffer, J., & van Speybroeck, L. 1982, *ApJ*, 259, L57
- Huchra, J., Brodie, J. P., & Kent, S. M. 1991, *ApJ*, 370, 495
- Ibata, R., Chapman, S., Ferguson, A. M. N., Lewis, G., Irwin, M., & Tanvir, N. 2005, *ApJ*, 634, 287
- Jablonka, P., Courbin, F., Meylan, G., Sarajedini, A., Bridges, T. J., & Magain, P. 2000, *A&A*, 359, 131
- Jiang, L., Ma, J., Zhou, X., Chen, J., Wu, H., & Jiang, Z. 2003, *AJ*, 125, 727
- Jordan, A., Cote, P., West, M. J., Marzke, R. O. 2002, *ApJ*, 576, L113
- Kaviraj, S., Rey, S.-C., Rich, R. M., Lee, Y.-W., Yoon, S.-J., & Yi, S. K. 2006, preprint (astro-ph/0601050)
- Kent, S. M., Huchra, J. P., & Stauffer, J. 1989, *AJ*, 98, 2080
- Larsen, S. S. 2004, in *The Formation and Evolution of Massive Young Star Clusters*, ed. H. J. G. L. M. Lamers, L. J. Smith, & A. Nota (San Francisco: ASP), 19

- Larsen, S. S., & Richtler, T. 1999, *A&A*, 345, 59
- Lee, H.-c., & Worthey, G. 2005, *ApJS*, 160, 176
- Lee, H.-c., Yoon, S.-J., & Lee, Y.-W. 2000, *AJ*, 120, 998
- Lee, H.-c., Lee, Y.-W., & Gibbson, B. K. 2002, *AJ*, 124, 2664
- Lee, H.-c., Lee, Y.-W., & Gibbson, B. K. 2003, in *Extragalactic Globular Cluster Systems*, ed. M. Kissler-Patig (Berlin: Springer), 261
- Lee, Y.-W., Demarque, P., & Zinn, R. J. 1994, *ApJ*, 423, 248
- Lee, Y.-W., et al. 2005, *ApJ*, 621, L57
- Maraston, C., Greggio, L., Renzini, A., Ortolani, S., Saglia, R. P., Puzia, T. H., & Kissler-Patig, M. 2003, *A&A*, 400, 823
- Martin, D. C., et al. 2005, *ApJ*, 619, L1
- Moehler, S. & Sweigart, A. V. 2006, preprint (astro-ph/0606054)
- Monet, D., et al. 2003, *AJ*, 125, 984
- Morrison, H. L., Harding, P., Perrett, K., & Hurley-Keller, D. 2004, *ApJ*, 603, 87
- Morrissey, P., et al. 2005, *ApJ*, 619, L7
- O’Connell, R. W. 1999, *ARA&A*, 37, 603
- Oke, J. B. 1990, *AJ*, 99, 1621
- Park, J.-H., & Lee, Y.-W. 1997, *ApJ*, 476, 28
- Perrett, K. M., Bridges, T. J., Hanes, D. A., et al. 2002, *AJ*, 123, 2490
- Peterson, R. C., Carney, B. W., Dorman, B., Green, E. M., Landsman, W., Liebert, J., O’Connell, R. W., Rood, R. T. 2003, *ApJ*, 588, 299
- Piotto, G., Sosin, C., King, I. R., et al. 1997, in *Advances in Stellar Evolution*, ed. R. T. Rood & A. Renzini (Cambridge: Cambridge Univ. Press), p. 84
- Puzia, T. H., Perrett, K. M., & Bridges, T. J. 2005, *A&A*, 434, 909
- Racine, R. 1991, *AJ*, 101, 865
- Reed, L. G., Harris, G. L. H., & Harris, W. E. 1994, *AJ*, 107, 555
- Rey, S.-C., Yoon, S.-J., Lee, Y.-W., Chaboyer, B., & Sarajedini, A. 2001, *AJ*, 122, 3219
- Rey, S.-C., Rich, R. M., et al. 2005, *ApJ*, 619, L119 (Paper I)
- Rich, R. M. 2004, in *Origin and Evolution of the Elements*, eds. A. McWilliam and M. Rauch (Cambridge: Cambridge Univ. Press), 255

- Rich, R. M., Minniti, D., & Liebert, J. 1993, *ApJ*, 406, 489
- Rich, R. M., Mighell, K. J., Freedman, W. L., & Neill, J. D. 1996, *AJ*, 111, 768
- Rich, R. M., et al. 1997, *ApJ*, 484, L23
- Rich, R. M., et al. 2005, *AJ*, 129, 2670
- Rose, J. A. 1984, *AJ*, 89, 1238
- Rose, J. A. 1985, *AJ*, 90, 1927
- Salaris, M., & Weiss, A. 2002, *A&A*, 388, 492
- Schiavon, R. P., Rose, J. A., Courteau, S., & MacArthur, L. A. 2004, *ApJ*, 608, L33
- Sarajedini, A., Chaboyer, B., & Demarque, P. 1997, *PASP*, 109, 1321
- Searle, L. 1978, *NATO Advanced Study Institute on Globular Clusters* (Cambridge: Cambridge Univ. Press)
- Sohn, S. T., et al. 2006, *AJ*, 131, 866
- Stetson, P. B. 1987, *PASP*, 99, 191
- Stephens, A. W., et al. 2001, *AJ*, 121, 2597
- Thilker, D. A. et al. 2005a, *ApJ*, 619, L67
- Thilker, D. A. et al. 2005b, *ApJ*, 619, L79
- Thomas, D., Maraston, C., & Bender, R. 2003, *MNRAS*, 339, 897
- Trager, S. C., Worthey, G., Faber, S. M., & Dressler, A. 2005, *MNRAS*, 362, 2
- van den Bergh, S. 1967, *AJ*, 72, 70
- van den Bergh, S. 1969, *ApJS*, 19, 145
- Vetevnik, M. 1962, *Bull. Astron. Inst. Czechoslovakia*, 13, 180
- Williams, B. F. & Hodge, P. W. 2001a, *ApJ*, 548, 190
- Williams, B. F. & Hodge, P. W. 2001b, *ApJ*, 559, 851
- Yi, S. 2003, *ApJ*, 582, 202
- Yi, S., Lee, Y.-W., Woo, J.-H., Park, J.-H., Demarque, P., & Oemler, A. Jr. 1999, *ApJ*, 513, 128

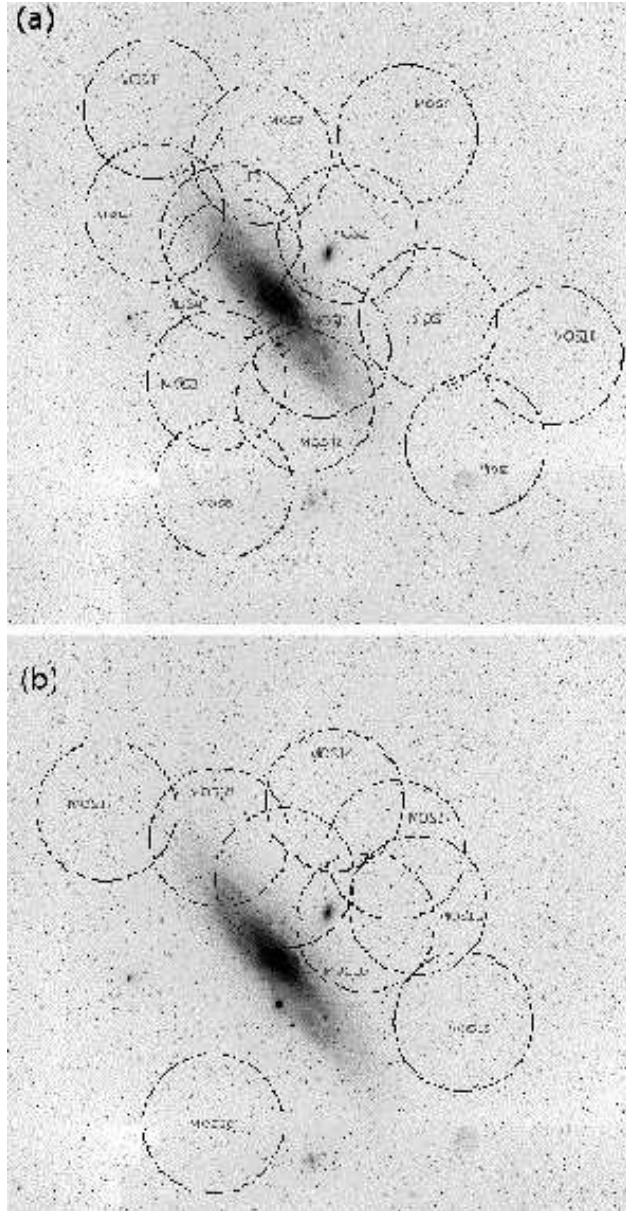


Fig. 1.— (a) 14 *GALEX* fields observed in 2003 and (b) additional 9 *GALEX* fields observed in 2004 projected onto a $6^\circ \times 6^\circ$ DSS image. North is to the top and East is to the left.

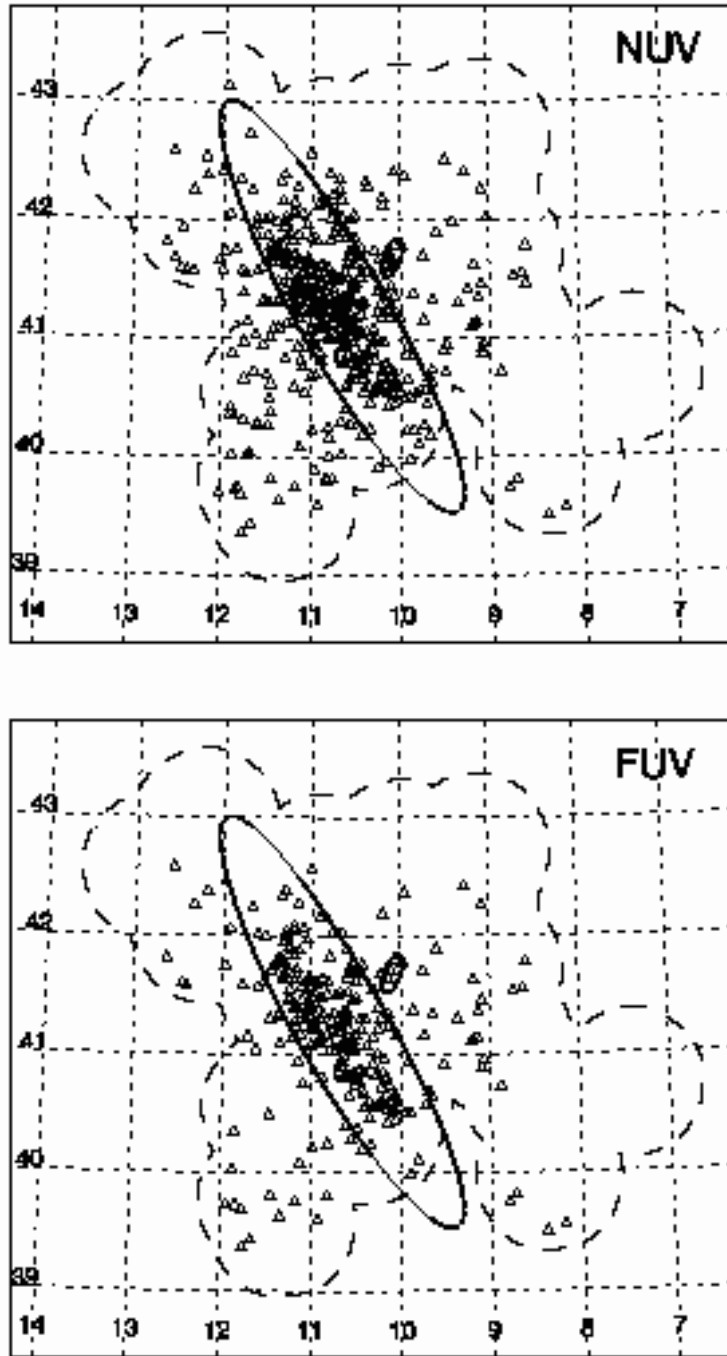


Fig. 2.— Spatial distribution on the sky of objects detected in *GALEX* NUV and FUV fields. The large ellipse in solid line is the disk/halo criterion for M31 defined by Racine (1991); two smaller ellipses are the D_{25} isophotes of NGC 205 (*larger*) and M32 (*smaller*). The boundary in dashed line shows the entire field covered by *GALEX* observations.

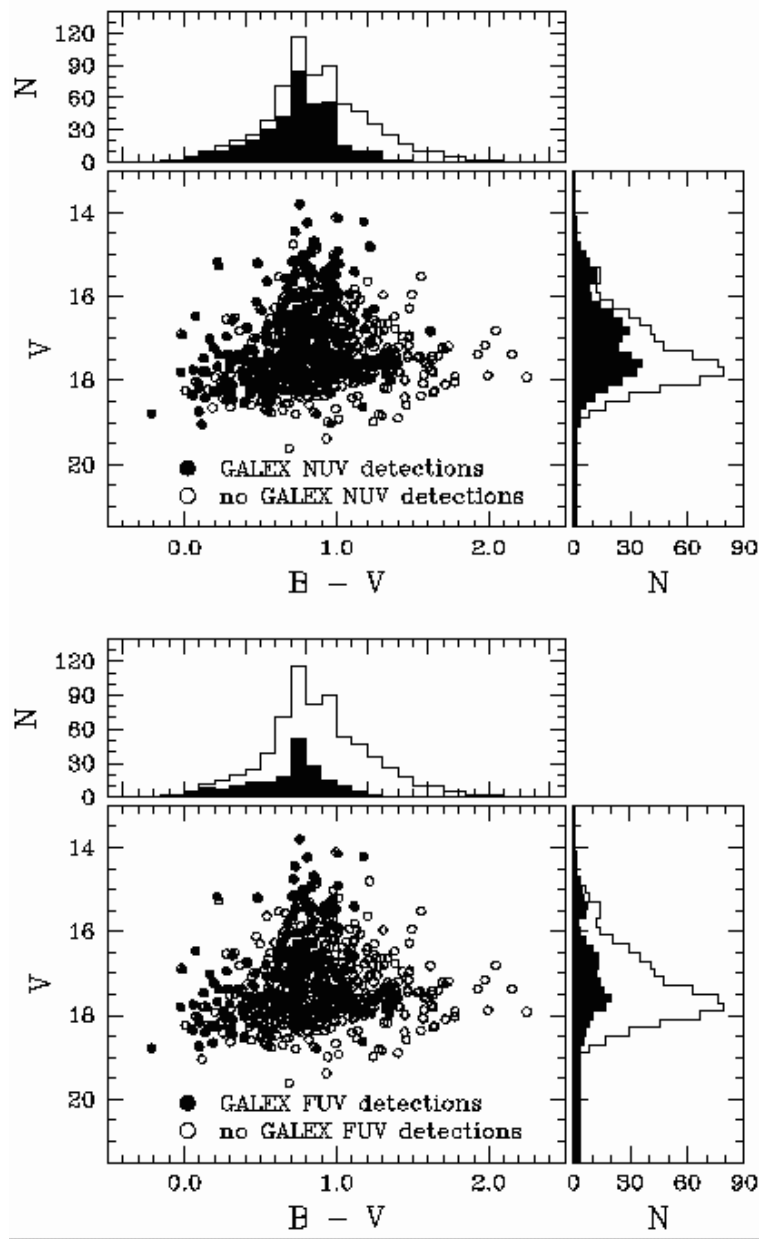


Fig. 3.— *GALEX* detection rates in NUV (*upper*) and FUV (*lower*). Of the 693 objects with both B and V data in RBC, 485 (about 70%) and 273 (about 39%) objects have their entries in the *GALEX* UV catalog for NUV and FUV, respectively.

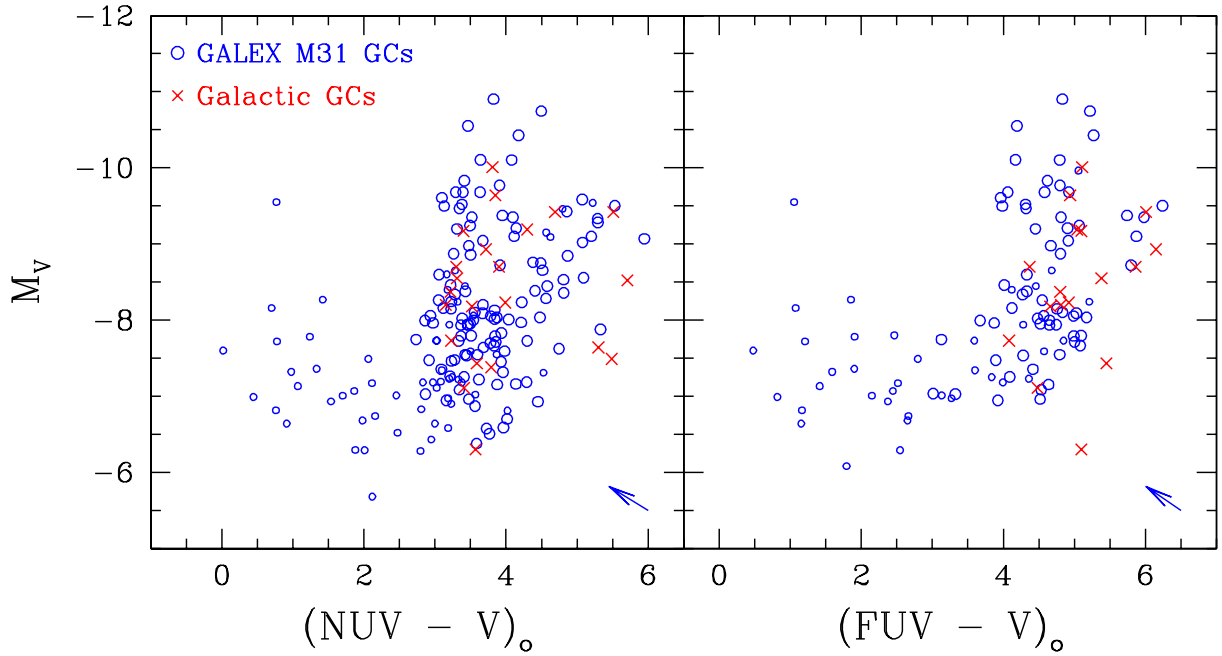


Fig. 4.— M_V vs. $(UV - V)_0$ color-magnitude diagrams for *GALEX* M31 GCs (*circles*). Only confirmed M31 GCs in RBC entries (i.e., class 1) are selected. Large circles are GCs with $E(B - V) < 0.16$ from Barmby et al. (2000). Small circles are GCs with no available reddening information in Barmby et al., assuming that they are only affected by the foreground Galactic reddening of $E(B - V) = 0.10$. *GALEX* M31 GCs are compared with Galactic GCs obtained from OAO-2 and ANS (*crosses*; Sohn et al. 2006). Relatively red GCs [$(NUV - V)_0 \geq 3.0$ and $(FUV - V)_0 \geq 4.0$] in M31 and old Galactic GCs occupy the same area in CMDs. Blue clusters [$(NUV - V)_0 \leq 3.0$ and $(FUV - V)_0 \leq 4.0$] are young cluster candidates (see text). The arrow indicates reddening vector by an increase of $E(B - V) = 0.10$.

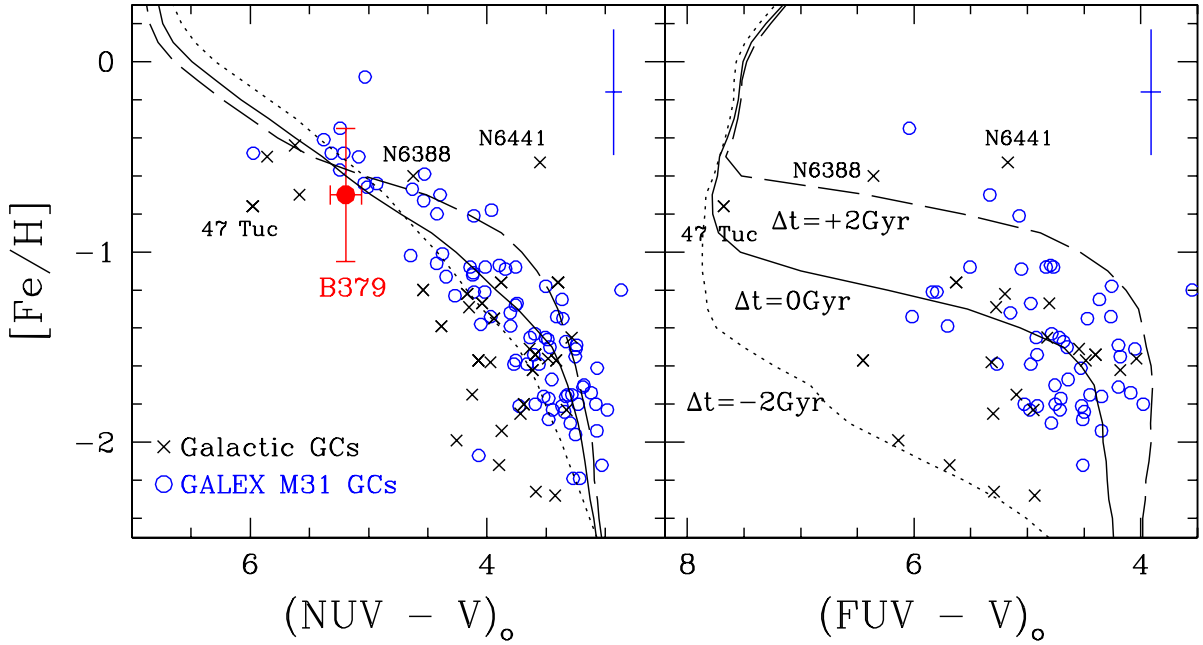


Fig. 5.— $[\text{Fe}/\text{H}]$ vs. $(UV - V)_0$ diagrams for M31 (*open circles*) and Galactic GCs (*crosses*; $[\text{Fe}/\text{H}]$ from Harris 1996). The model isochrones are constructed from our evolutionary population models of GCs in the *GALEX* filter system (Chung, Yoon, & Lee 2006, in preparation; see also Lee et al. 2002; Yi 2003). The $\Delta t = 0$ (*solid line*) isochrone corresponds to inner halo Galactic GCs (Galactocentric radius ≤ 8 kpc) of ~ 12 Gyr. The $\Delta t = +2$ Gyr (*long dashed line*) and -2 Gyr (*dotted line*) isochrones are for the models 2 Gyr older and younger than the inner halo Galactic GCs, respectively. Typical errors of $[\text{Fe}/\text{H}]$ [calculated from column (20) of Table 2] and colors of M31 GCs are shown as error bars. Cluster B379, an M31 GC with direct age estimation by Brown et al. (2004), is shown as a filled circle.

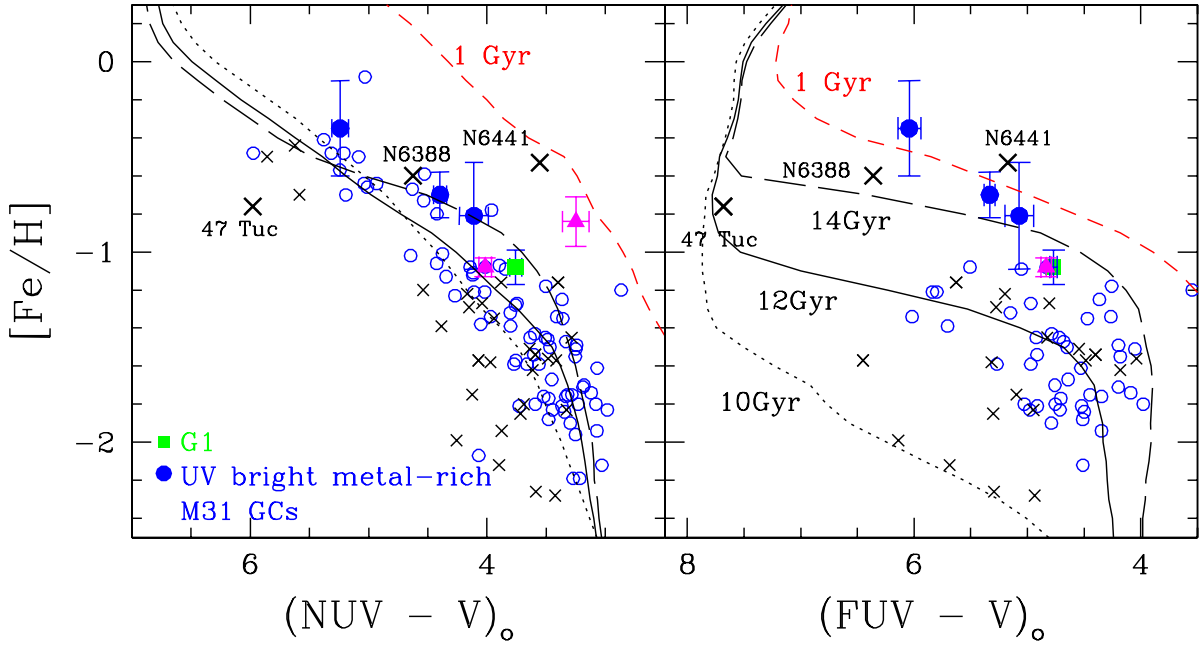


Fig. 6.— $[\text{Fe}/\text{H}]$ vs. $(UV - V)_0$ diagrams for UV bright metal-rich GCs in M31 (*filled circles*). Three metal-rich ($[\text{Fe}/\text{H}] > -1.0$) M31 GCs show significant FUV flux comparable to those of peculiar metal-rich Galactic GCs, NGC 6388 and NGC 6441, with anomalous hot HB stars. The filled triangles indicates metal-rich M31 GCs (B158 and B234) that may be analogs of NGC 6388 and NGC 6441 suggested by Beasley et al. (2005) from the results of Ca II index. The moderately metal-rich ($[\text{Fe}/\text{H}] = -1.08$) M31 GC G1 (*filled square*) shows relatively large UV flux which is consistent with its HB morphology with a notable minor population of blue HB stars. We also superpose a young (1 Gyr, *dashed line*) isochrone.

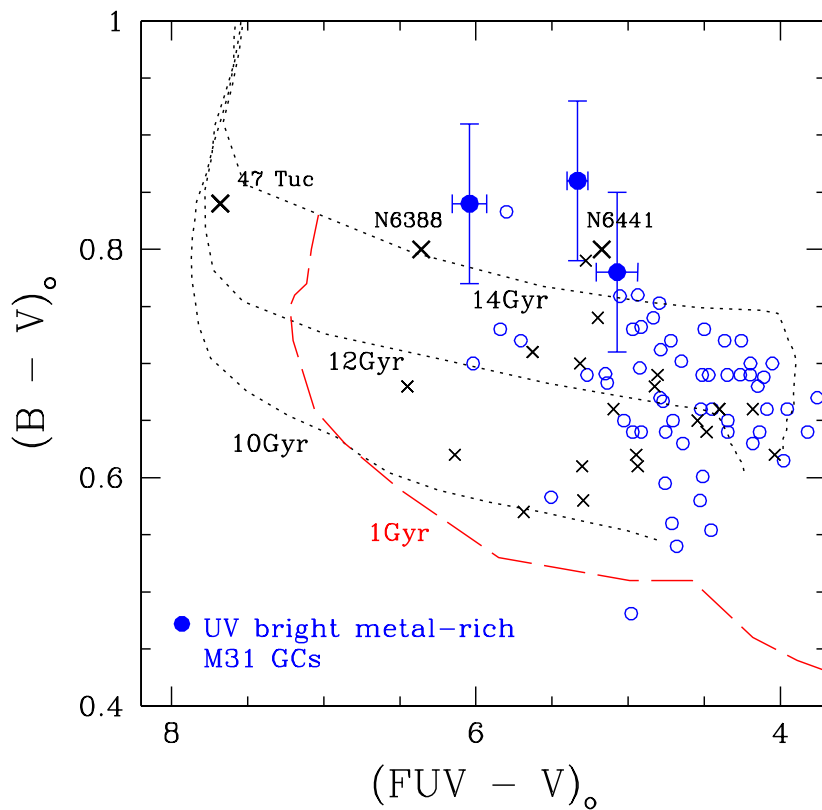


Fig. 7.— $(B - V)_0$ vs. $(FUV - V)_0$ diagram for UV bright metal-rich GCs in M31 (*filled circles*). The long dashed line is for the 1 Gyr isochrone. All candidate UV bright metal-rich GCs follow isochrones for old ages, which confirms that they are bona-fide old metal-rich GCs with large FUV flux. The $B - V$ and $FUV - V$ errors of the UV bright metal-rich GCs are estimated from the typical internal errors (0.05 mag) of B and V magnitudes suggested by Galleti et al. (2004).

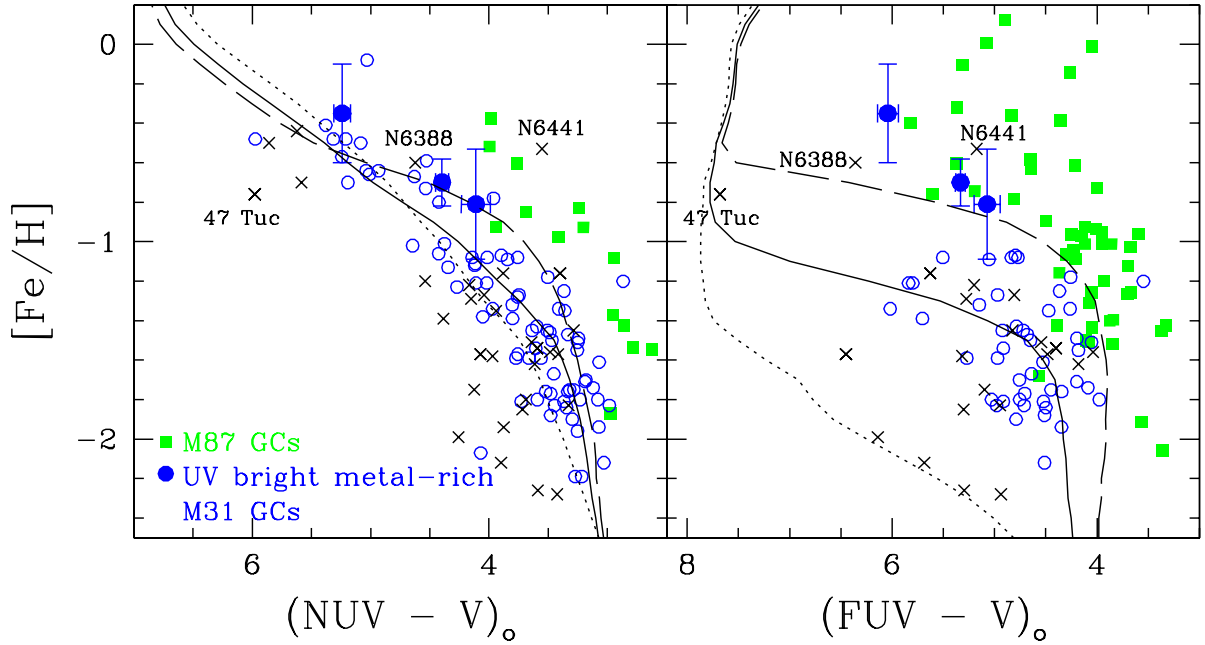


Fig. 8.— Comparison of UV bright metal-rich GCs in M31 (*filled circles*) with GCs in giant elliptical galaxy M87 (*filled squares*; Sohn et al. 2006). Most M87 GCs are systematically UV bright at a fixed $[\text{Fe}/\text{H}]$, compared to the Milky Way (*crosses*) and M31 (*circles*) GCs. It is worth to note that metal-rich UV bright GCs in M31 and Galactic counterparts, NGC 6388 and NGC 6441, fall in the vicinity of the distribution of metal-rich M87 GCs in $[\text{Fe}/\text{H}]$ vs. $(FUV - V)_0$ diagram. This suggests that UV bright metal-rich GCs in M31 and Milky Way may share their properties with metal-rich GCs in M87.

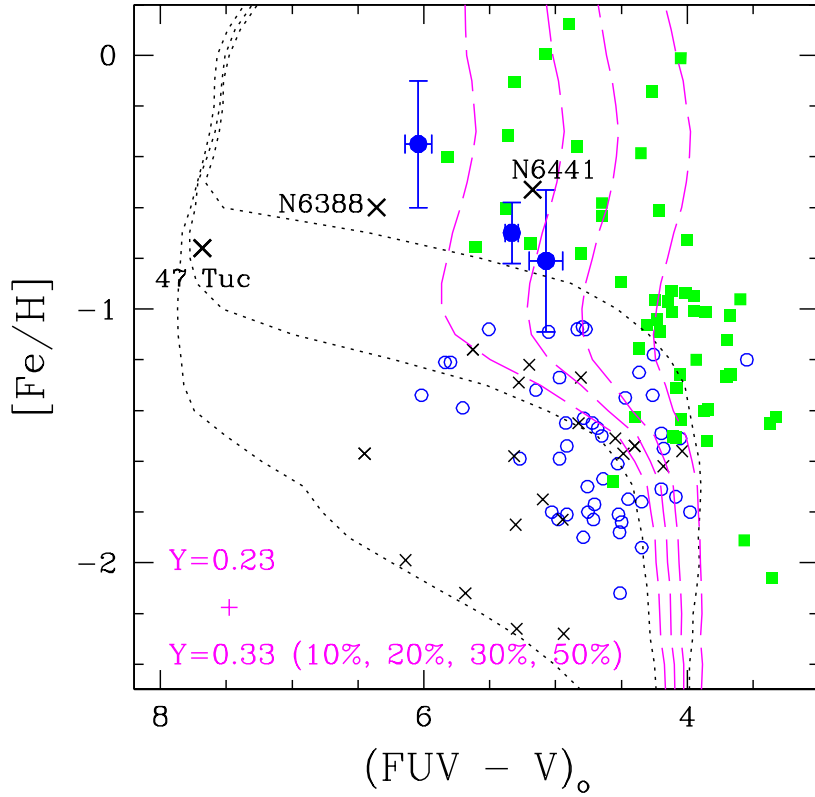


Fig. 9.— Comparison of UV bright metal-rich GCs in M31 (*filled circles*) and M87 (*filled squares*; Sohn et al. 2006) with the model predictions. Dotted lines are for the case in which all the GCs have same primordial helium abundance of $Y = 0.23$ but different ages. Dashed lines are for the case with minority population of helium enhancement ($Y = 0.33$) in addition to the majority of the population with normal helium abundance ($Y = 0.23$) within a model GC at the same age of 12 Gyr. Different dashed lines indicate GCs with different subpopulation number fraction of helium enhancement (left to right, 10%, 20%, 30%, and 50%) within a GC. A reasonable agreement between observed UV colors of metal-rich GCs and models is obtained when we adopt a large range of helium abundance.

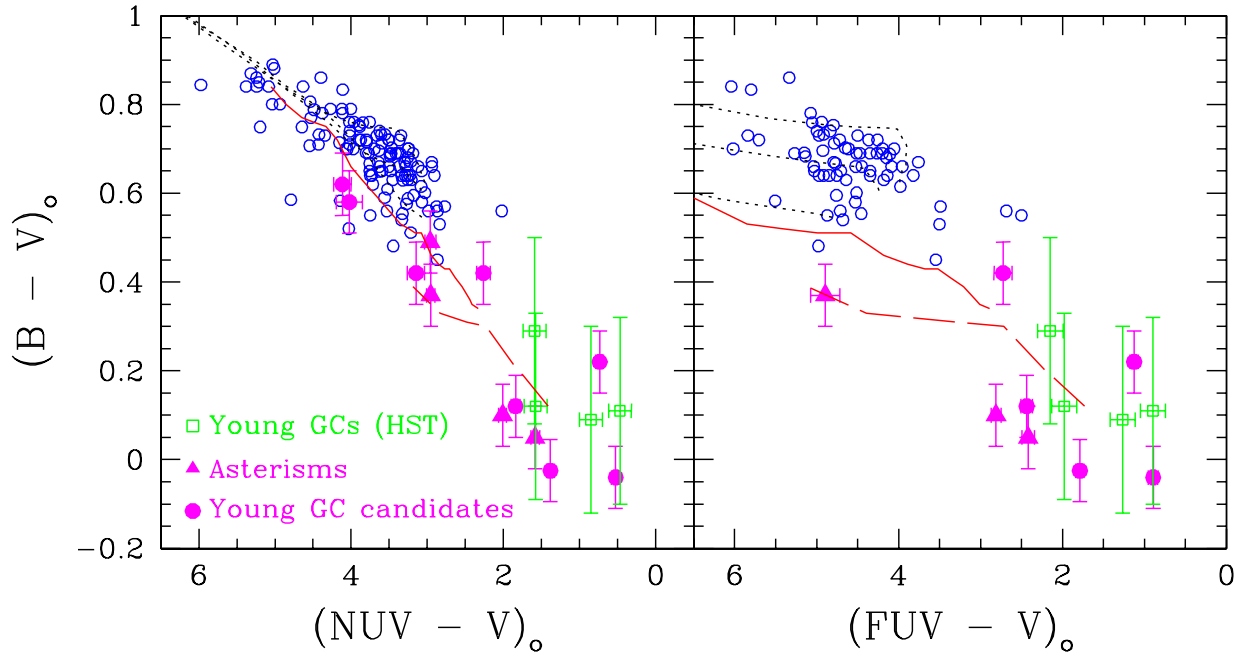


Fig. 10.— $(B - V)_0$ vs. $(UV - V)_0$ diagrams for young GCs. Filled circles are young GCs found from the recent high-quality spectroscopic observations (Beasley et al. 2004; Burstein et al. 2004). We adopt $E(B - V) = 0.10$ for these clusters. The spectroscopically determined ages of young GCs are in good agreement with our population models in the range of 0.5 Gyr (*long dashed line*) – 1 Gyr (*solid line*). Open squares are young GCs observed by Williams & Hodge (2001a) with *HST*. Filled triangles are probable asterisms suggested by Cohen et al. (2005). Open circles are possible old GCs in M31 and dotted lines are our model isochrones in the range of 10 Gyr – 14 Gyr.

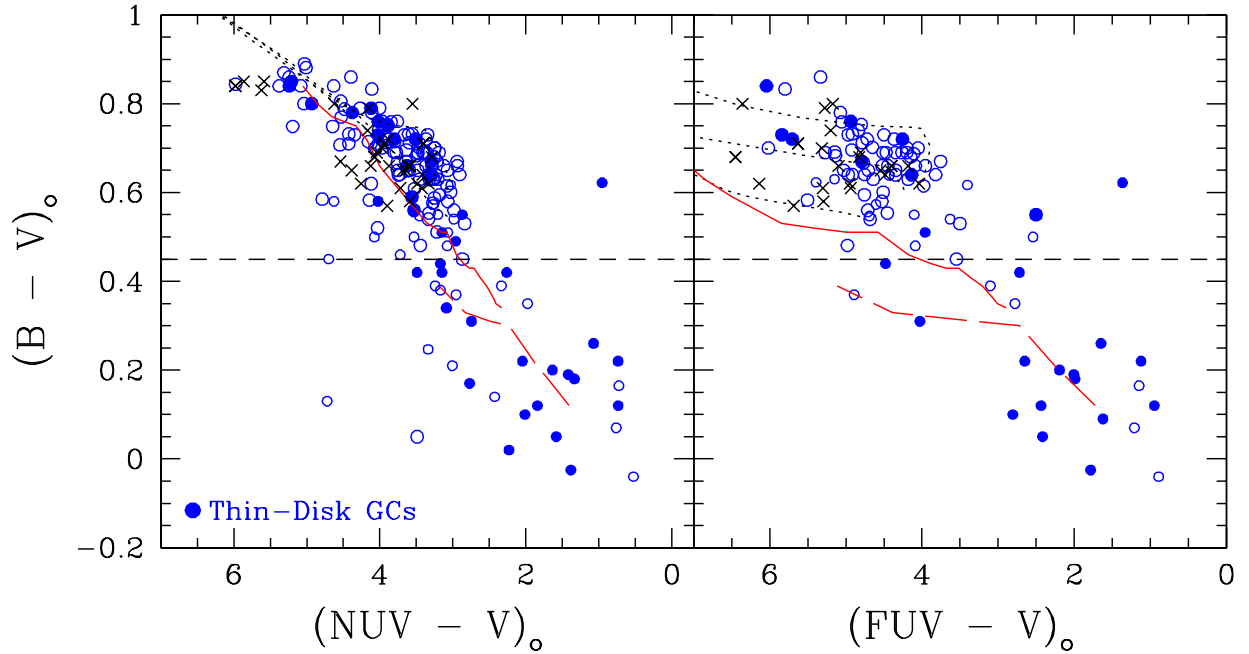


Fig. 11.— $(B - V)_0$ vs. $(UV - V)_0$ diagrams for M31 GCs with thin-disk kinematics (*filled circles*) from Morrison et al. (2004). We superpose our model isochrones of 1 Gyr (*solid line*) and 0.5 Gyr (*long dashed line*). Dotted lines are our model isochrones in the range of 10 Gyr – 14 Gyr. The dashed horizontal line corresponds to the reference value of $(B - V)_0 = 0.45$ for young GC selection adopted from Fusi Pecci et al. (2005). Large fraction of thin-disk GCs with $(B - V)_0 < 0.45$ show young ages with less than 1 Gyr. At the same time, small fraction of thin-disk GCs with $(B - V)_0 > 0.45$ appear to be old.

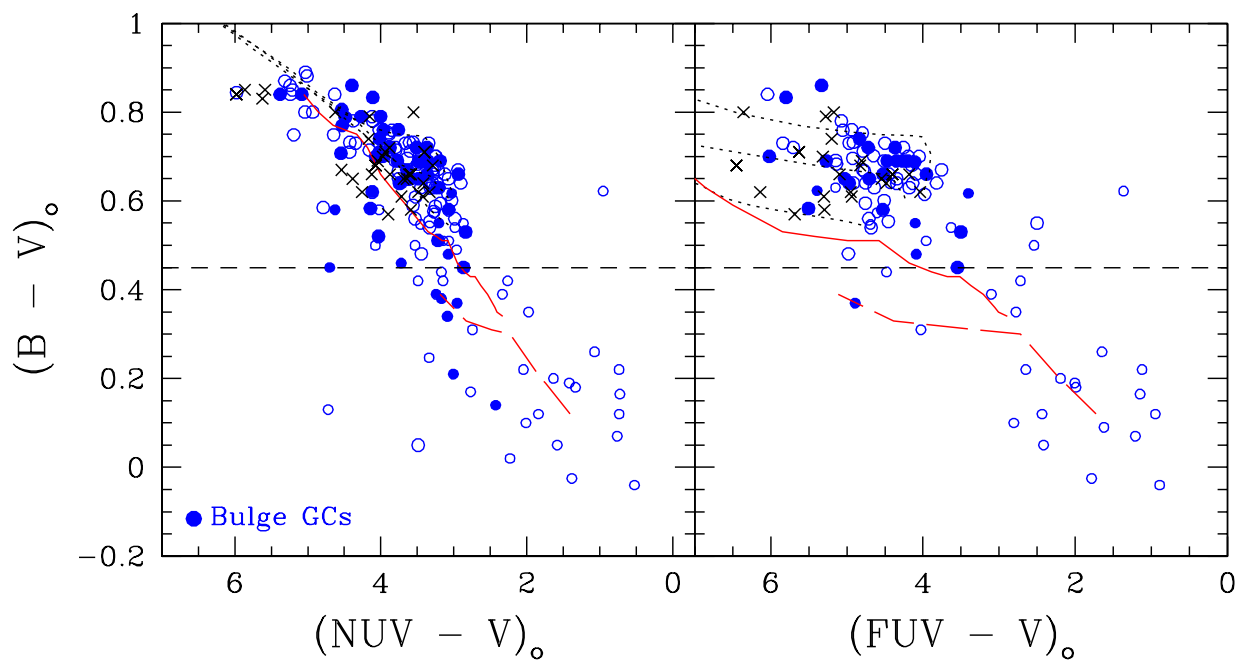


Fig. 12.— Same as Fig. 11, but for M31 GCs with bulge kinematics (*filled circles*) from Morrison et al. (2004). Contrary to the thin-disk GCs, bulge GCs are biased to the relatively red optical/UV colors which indicates the mean age of bulge GCs is old. The age distribution of bulge GCs support most of blue GCs [$(B - V)_0 < 0.45$] without kinematic data are possible thin-disk clusters.

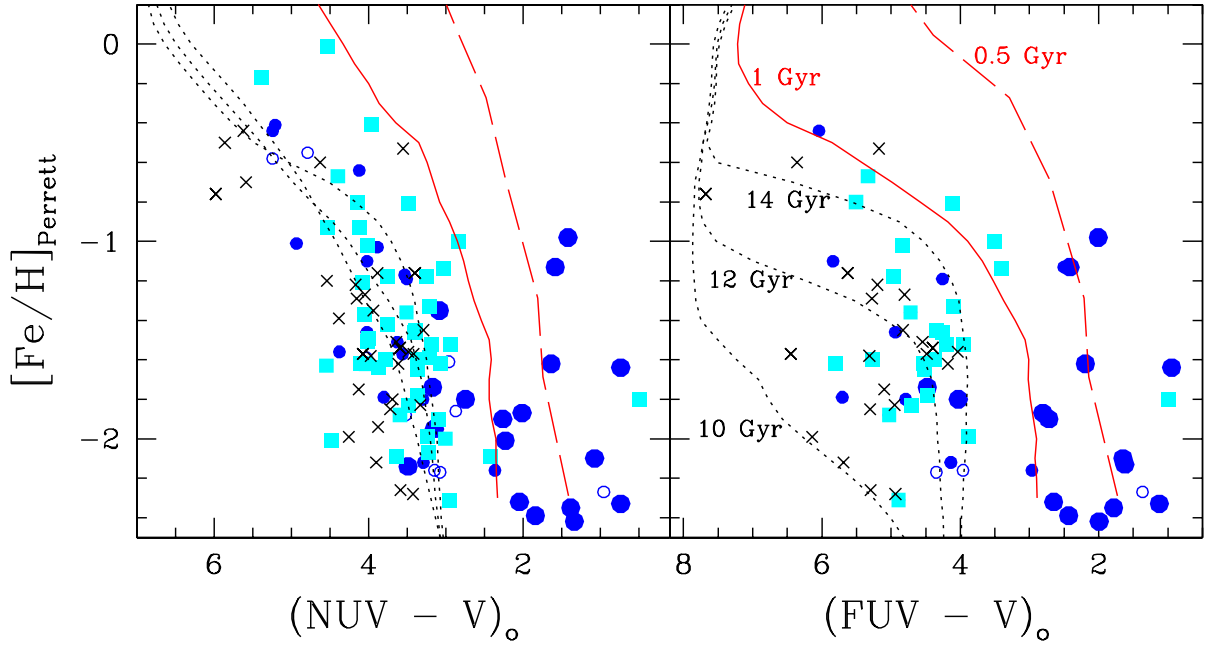


Fig. 13.— $[\text{Fe}/\text{H}]$ vs. $(UV - V)_0$ diagrams for thin-disk GCs (*filled circles*) and bulge GCs (*filled squares*) in M31. In addition to the model isochrones with old ages comparable to mean Galactic halo (10 – 14 Gyr, *dotted lines*), we also superpose our young isochrones of 1 Gyr (*solid line*) and 0.5 Gyr (*long dashed line*). Optically blue thin-disk GCs [$(B - V)_0 < 0.45$; *large filled circles*] show systematically stronger UV flux than do red thin-disk GCs [$(B - V)_0 > 0.45$; *small filled circles*] at a given metallicity. This is consistent with that the blue thin-disk GCs are systematically young GCs with < 1 Gyr. GCs with bulge kinematics are biased to the red UV color distribution, which is an indication of their old ages. Since $[\text{Fe}/\text{H}]$ values of Barmby et al. are not available for many thin-disk GCs of Morrison et al. (2004), we instead adopt $[\text{Fe}/\text{H}]$ from Perrett et al (2002).

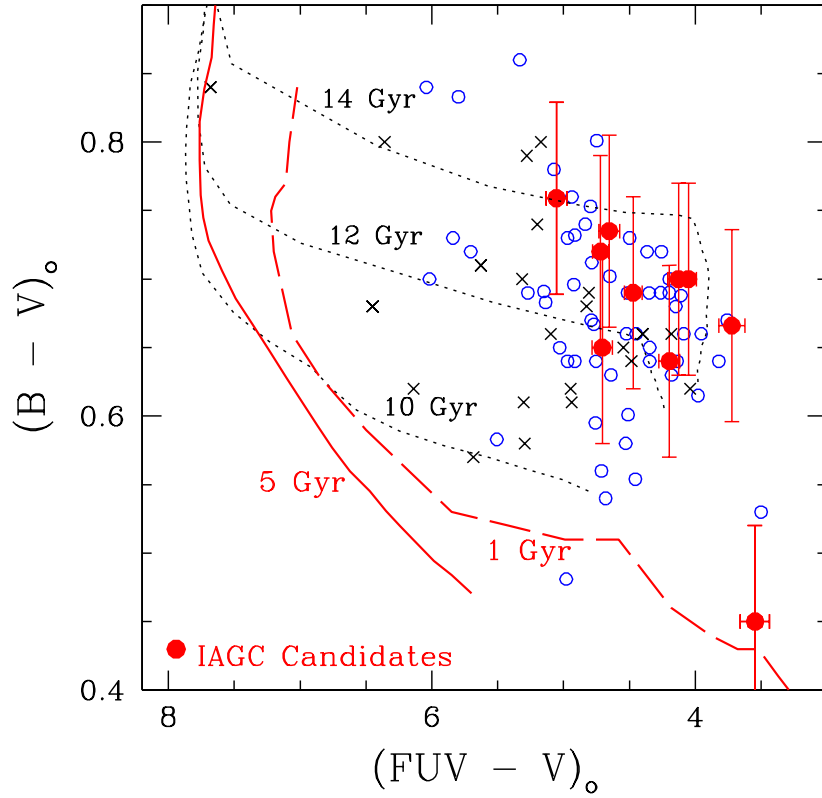


Fig. 14.— Comparison of spectroscopically classified intermediate-age GC candidates (*filled circles*) with the model predictions. Superposed are our model isochrones for old (10, 12, and 14 Gyr; *dotted lines*), intermediate (5 Gyr; *solid line*), and young (1 Gyr; *long dashed line*) ages. All but one intermediate-age GC candidates detected in FUV are placed in the color-color diagram generally occupied by old GCs of age with 12 – 14 Gyr.

Table 1. Position of *GALEX* M31 Additional Fields

Field	RA (2000)	DEC (2000)	Exposure (s)
M31-MOS13	00 36 00.00	41 45 00.00	1620
M31-MOS14	00 40 00.00	42 42 00.00	2338
M31-MOS15	00 33 55.20	40 42 00.00	3241
M31-MOS16	00 38 31.20	41 36 00.00	5113
M31-MOS17	00 42 24.00	42 00 00.00	5108
M31-MOS18	00 45 36.00	42 21 36.00	3251
M31-MOS19	00 51 07.20	42 34 12.00	3231
M31-MOS20	00 45 40.80	39 47 06.00	1456
M31-MOS21	00 37 01.20	42 15 00.00	1357

Table 2. UV and optical photometry of M31 globular clusters and candidates

ID	Alt. ID	NED ID	Flag	RA (J2000)	DEC (J2000)	m_{NUV}	σ_{NUV}	m_{FUV}	σ_{FUV}	U	B
G001	000-001	SKHV 001	1	00:32:46.51	+39:34:39.7	18.015	0.012	18.972	0.031	...	14.56
G002	000-002	SKHV 002	1	00:33:33.79	+39:31:18.5	19.383	0.023	20.911	0.079	16.75	16.48
B289	...	Bol 289	1	00:34:20.85	+41:47:50.9	19.861	0.030	21.140	0.092	17.00	16.76
B290	290-000	Bol 290	1	00:34:20.86	+41:28:17.9	22.500	0.116	18.46	18.04
B411	...	Bol 411	2	00:34:30.83	+41:33:43.8	20.753	0.035	21.361	0.074	18.59	18.81
BA21	...	[BA64] 3-21	2	00:34:54.01	+39:49:41.5	20.954	0.054	21.774	0.124	17.56	17.53
B412	...	Bol 412	2	00:34:55.22	+41:32:25.5	21.754	0.067	22.299	0.190	18.93	18.43
BA22	...	[BA64] 3-22	2	00:35:13.77	+39:45:38.3	21.467	0.074	21.840	0.131
B134D	...	Bol D134	2	00:35:30.33	+40:44:26.1	20.785	0.028	21.608	0.069	18.46	18.65
B291	291-009	Bol 291	1	00:36:04.87	+42:02:09.8	20.916	0.039	17.65	17.34
B292	292-010	Bol 292	1	00:36:16.59	+40:58:26.6	21.018	0.033	21.796	0.085	17.87	17.89
B414	...	Bol 414	2	00:36:19.31	+42:16:30.6	20.611	0.023	20.998	0.043	18.56	18.48
B293	293-011	Bol 293	1	00:36:20.78	+40:53:36.6	20.141	0.021	21.174	0.057	17.19	17.03
B137D	...	Bol D137	2	00:36:20.90	+40:55:59.6	22.272	0.082	19.00	19.05
B138D	...	Bol D138	2	00:36:21.67	+41:28:32.6	22.380	0.064	23.110	0.176	18.70	17.92

*The complete version of this table is in the electronic edition of the Journal. The printed edition contains only a sample.